AWARD NUMBER: W81XWH-15-1-0296

TITLE: Targeting MEK5 Enhances Radiosensitivity of Human Prostate Cancer and Impairs Tumor-Associated Angiogenesis

PRINCIPAL INVESTIGATOR: Constantinos G. Broustas, PhD

CONTRACTING ORGANIZATION: Columbia University
New York, NY 10032

REPORT DATE: December 2019

TYPE OF REPORT: Final

PREPARED FOR: U.S. Army Medical Research and Materiel Command
Fort Detrick, Maryland 21702-5012

# REPORT DOCUMENTATION PAGE

*Form Approved*
*OMB No. 0704-0188*



| 1. REPORT DATE | 2. REPORT TYPE | 3. DATES COVERED |
|---|---|---|
| Dec 2019 | Final | 08/31/2015 - 08/30/2019 |

**4. TITLE AND SUBTITLE**

Targeting MEK5 Enhances Radiosensitivity of Human Prostate Cancer and Impairs Tumor-Associated Angiogenesis

**5a. CONTRACT NUMBER**

**5b. GRANT NUMBER**
W81XWH-15-1-0296

**5c. PROGRAM ELEMENT NUMBER**

**6. AUTHOR(S)**

Constantinos G. Broustas

E-Mail: cgb2117@cumc.columbia.edu

**5d. PROJECT NUMBER**

**5e. TASK NUMBER**

**5f. WORK UNIT NUMBER**

**7. PERFORMING ORGANIZATION NAME(S) AND ADDRESS(ES)**

Columbia University
New York, NY 10032

**8. PERFORMING ORGANIZATION REPORT NUMBER**

**9. SPONSORING / MONITORING AGENCY NAME(S) AND ADDRESS(ES)**

U.S. Army Medical Research and Materiel Command
Fort Detrick, Maryland 21702-5012

**10. SPONSOR/MONITOR'S ACRONYM(S)**

**11. SPONSOR/MONITOR'S REPORT NUMBER(S)**

**12. DISTRIBUTION / AVAILABILITY STATEMENT**
Approved for Public Release; Distribution Unlimited

**13. SUPPLEMENTARY NOTES**

**14. ABSTRACT**

Radiotherapy is commonly used to treat a variety of solid human tumors, including localized prostate cancer. However, treatment failure often ensues due to tumor intrinsic or acquired radioresistance. We find that the MEK5/ERK5 signaling pathway is associated with resistance to genotoxic stress in aggressive prostate cancer cells. MEK5 knockdown by RNA interference sensitizes prostate cancer cells to ionizing radiation (IR) and etoposide treatment, as assessed by clonogenic survival and short-term proliferation assays. Mechanistically, MEK5 downregulation impairs phosphorylation of the catalytic subunit of DNA-PK at serine 2056 in response to IR or etoposide treatment. Although MEK5 knockdown does not influence the initial appearance of radiation- and etoposide-induced γH2AX and 53BP1 foci, it markedly delays their resolution, indicating a DNA repair defect. A cell-based assay shows that non-homologous end joining (NHEJ) is compromised in cells with ablated MEK5 protein expression. Finally, MEK5 silencing combined with focal irradiation causes strong inhibition of tumor growth in mouse xenografts, compared with MEK5 depletion or radiation alone. These findings reveal a convergence between MEK5 signaling and DNA repair by NHEJ in conferring resistance to genotoxic stress in advanced prostate cancer and suggest targeting MEK5 as an effective therapeutic intervention in the management of this disease.

**15. SUBJECT TERMS**
MEK5, DNA-PKcs, non-homologous end-joining, ionizing radiation, prostate cancer

| 16. SECURITY CLASSIFICATION OF: | | | 17. LIMITATION OF ABSTRACT | 18. NUMBER OF PAGES | 19a. NAME OF RESPONSIBLE PERSON |
|---|---|---|---|---|---|
| a. REPORT | b. ABSTRACT | c. THIS PAGE | | | USAMRMC |
| Unclassified | Unclassified | Unclassified | Unclassified | 26 | 19b. TELEPHONE NUMBER *(include area code)* |

Table of Contents

**Page**

## INTRODUCTION

Radiation is the most critical therapeutic modality for treating human prostate cancer. However, tumor recurrence and therapy resistance often ensue. Moreover, radiation is not free of other serious unwanted risks, including the promotion of secondary cancer (1), as well as increased tumor-associated angiogenesis and metastasis, especially when cells are subjected to sublethal doses of radiation. A major cause of failure in radiation treatment is intrinsic and therapy-induced radioresistant tumor cells. The major mechanisms for radiotherapeutic resistance are the DNA damage and repair pathway, as well as cell membrane-associated prosurvival pathways such as EGF receptor and phosphoinositide 3-kinase (PI3K)/AKT. Although the delivery of higher doses of ionizing radiation improves local control (2-4), there are constraints due to dose-limiting toxicities to noncancerous tissues (5-7). Thus, lowering radiation dose, while preserving therapeutic index, is a goal in both the laboratory research setting and the clinic.

Mitogen-activated protein kinase kinase 5 (MAP2K5 or MEK5), belongs to the family of MAP kinases. It is activated by the upstream kinases MEKK2 and MEKK3 at S311/T315, or in some cases directly by c-Src (8-11). MEK5, in turn, phosphorylates and activates extracellular signal-regulated kinase 5 (ERK5 or BMK1) at T218/Y220 (8). Targeted deletion of *Mek5* or *Erk5* genes in mice is embryonic lethal due to defects in blood vessel formation and cardiac development (12-14). Initial vascularization in *Erk5*$^{-/-}$ embryos occurs normally; however, subsequent remodeling and/or maintenance of vasculature (angiogenesis) is adversely affected by the absence of ERK5 (15). Most importantly, the MEK5/ERK5 signaling pathway is essential for tumor-associated angiogenesis (16). Tumor xenografts growing in *Erk5* knockout mice show a significantly reduced vascular density and tumor growth than growing in *Erk5* wild type mice (16).

The MEK5/ERK5 pathway can be activated by various stimuli such as oxidative stress, growth factors, and mitogens downstream of receptor tyrosine kinases, and G protein-coupled receptors, and culminates in the activation of a large number of transcription factors, including MEF2 (myocyte enhancer factor 2), c-JUN, NF-κB, CREB, and transcription factors that control the epithelial-mesenchymal transition (EMT) program (17-22). Moreover, gene expression analysis has shown that the MEK5/ERK5 pathway may also control hypoxia-responsive genes by a mechanism independent of HIF-1α expression control, under normoxic conditions (23).

MEK5/ERK5 pathway plays a pivotal role in tumor initiation and progression, including prostate cancer. MEK5 protein is overexpressed in prostate cancer cells compared with normal cells and MEK5 levels are correlated with prostate cancer metastasis (24). Furthermore, high expression of ERK5 in prostate cancer has also been found to correlate with poor disease-specific survival and could serve as an independent prognostic factor (25) and ERK5 expression in prostate cancer is associated with an invasive phenotype (26).

This study demonstrates that MEK5 downregulation enhances radiosensitization in human prostate cancer cells. MEK5 silencing modulates the activation of DNA-PKcs, major player of the DNA repair pathway, and impairs non-homologous end-joining. Importantly, *in vivo* studies using a mouse xenograft model show that MEK5 ablation synergizes with radiation to suppress tumor growth.

## KEYWORDS

MEK5, DNA-PKcs, non-homologous end-joining, ionizing radiation, prostate cancer, xenograft model

## ACCOMPLISHMENTS

### What were the major goals of the project?

**Specific Aim 1**
**Task 1:** Prepare cell lines stably expressing shMEK5, HA-MEK5, HA-MEK5DD (constitutively active kinase). Cell lines to be used: DU145, PC3, EP156T

**Task 2:** Examine the effect of MEK5 downregulation on cell cycle progression, apoptosis, and DNA damage repair activation after treatment with ionizing radiation. Predictably induce radioresistance by ectopically expressing MEK5 in relatively radiosensitive prostate cell lines.

**Task 3:** MEK5 silencing combined with irradiation attenuates prostate tumor growth *in vivo*

**Specific Aim 2**
**Task 1:** Evaluate the contribution of AKT to MEK5-induced radioresistance by employing both an AKT-specific inhibitor and AKT specific siRNAs in MEK5-expressing cells and expressing an active AKT construct in prostate cancer cells with reduced MEK5 levels: Measure the effect on cell radioresistance by clonogenic survival. Cell lines to be used: DU145, PC3 [ATCC].

**Task 2:** Perform global gene expression analysis. Confirm by quantitative real time (qRT)-PCR.

**Specific Aim 3**
**Task 1:** *In vitro* studies (cell proliferation, migration, tube formation). Antibody arrays.

### What was accomplished under these goals?

(1) Prepared stable clones of MEK5 knockdown in PC3 and DU145 cells.
(2) Demonstrated that MEK5 depletion sensitizes DU145 and PC3 cells to ionizing radiation by both clonogenic survival assays, as well as cell proliferation assays.
(3) Discovered that MEK5 knockdown differentially regulates activation of DNA-PKcs, a major player in DNA repair, in response to genotoxic stress. Furthermore, MEK5 knockdown delays the resolution of IR or etoposide-induced double strand breaks by monitoring the formation and resolution of γH2AX and 53BP1 foci formation. Finally, a cell-based assay demonstrated that non-homologous end-joining is severely compromised in MEK5 depleted PC3 cells.
(4) Successfully completed the *in vivo* experiments with MEK5 knockdown and radiation.
(5) Demonstrated that MEK5 is required for AKT activation in response to ionizing radiation.
(6) Generated stable PC3 cells with reduced levels of MEK5, ectopically expressing activated AKT.
(7) Completed the DNA microarray experiments using shMEK5 alone or in combination with irradiation in PC3 and DU145 cells. We have identified differentially expressed genes and performed pathway analysis.
(8) Discovered that interleukin-1β (IL-1β), a pro-angiogenic factor, is controlled by MEK5 and, additionally, levels of endogenous and secreted IL-1β are increased by ionizing radiation.
(9) A manuscript describing part of the data has been accepted for publication in *Oncogene*.

**Specific Aim 1**

**Task 1:** Prepare cell lines stably expressing shMEK5.

We isolated several stable clones expressing *shControl* in both DU145 and PC3 cell lines, as well as two PC3 cell clones (#12, #22) expressing *shMEK5*. Knockdown in PC3/*shMEK5* cells is more than 90%. Now, we have also been able to isolate DU145 cells with *shMEK5* (#5, #7, and #9) with more than 80% reduction in MEK5 protein expression (**Figure 1**).

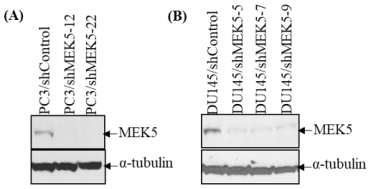


**Figure 1**: PC3 and DU145 clones stably expressing shMEK5. PC3 **(A)** and DU145 **(B)** cells were infected with lentiviral particles containing pLKO.1-shRNA against MEK5. PC3 clones (12, 22) and DU145 clones (5, 7, and 9) with shMEK5 knockdown were isolated after 1 μg/ml (PC3) or 0.4 μg/ml (DU145) puromycin selection.

**Task 2:** Examine the effect of MEK5 downregulation on cell cycle progression, apoptosis, and DNA damage repair activation after treatment with ionizing radiation. Predictably induce radioresistance by ectopically expressing MEK5 in relatively radiosensitive prostate cell lines.

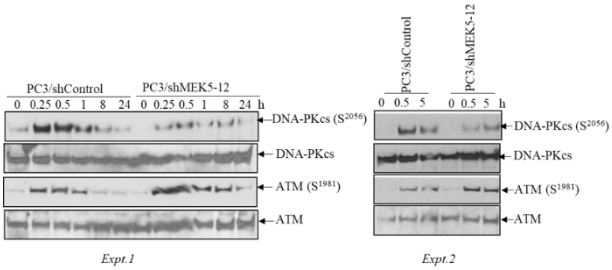


**Figure 2**: **MEK5 knockdown impairs DNA-PKcs phosphorylation.** PC3 cells stable expressing a control (shControl) or MEK5 (shMEK5-12) shRNA were exposed to 3 Gy of γ-rays and cells were lysed at the indicated times. Lysates were separated onto a 3-8% Tris-acetate buffer and immunoblotted sequentially with phospho-DNA-PKcs (Ser2056), total DNA-PKcs, phospho-ATM (Ser1981) and total ATM antibodies. Shown two independent experiments.

We determined the impact of ionizing radiation on MEK5/ERK5 pathway activation. Time course experiments with PC3 cells showed that IR resulted in phosphorylation of ERK5 at $T^{218}/Y^{220}$. In contrast, PC3 cells stably expressing shMEK5 did not show any phospho-ERK5 increase in response to IR (**Figure 2**). Furthermore, we demonstrated that MEK5 knockdown resulted in the radiosensitization of DU145, and PC3 cell lines as judged by long-term clonogenic survival analysis and short-term cell proliferation assays (**Figure 3**).

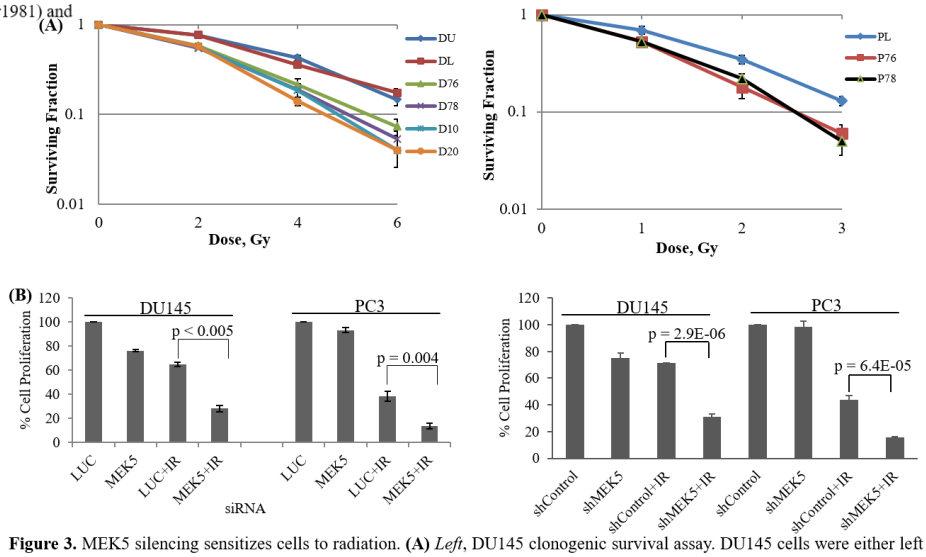


**Figure 3.** MEK5 silencing sensitizes cells to radiation. **(A)** *Left*, DU145 clonogenic survival assay. DU145 cells were either left untransfected (DU) or transiently transfected with luciferase siRNA (DL) or four different siRNAs against MEK5 (D76, D78, D10, D20). Two days later, cells were irradiated with increasing doses of γ-radiation and plated for clonogenic assay. *Right,* PC3 cells were transfected with luciferase siRNA (PL) as control or MEK5 siRNAs (P76, P78) and clonogenic assay was carried out. **(B)** Cell proliferation assay. *Left*, DU145 and PC3 cells were transiently transfected with control *Luciferase* (LUC) or *MEK5* siRNA. Three days later, cells were irradiated with 4 Gy γ-rays and incubated for 6 days. Cells were trypsinized and counted with a hemocytometer. *Right*, DU145 and PC3 cells were stably expressing either scrambled (shControl) or *MEK5* (shMEK5) shRNA were exposed to 4 Gy (DU145) or 3 Gy (PC3), or were sham irradiated. Data represent the mean ± S.D (n = 3). P-values were calculated by Student's t-test.

The DNA damage response and repair (DDR) signaling network is activated in response to genotoxic stress, including IR. We determined the impact of combining MEK5 depletion with IR on DNA repair. We discovered that depletion of MEK5 markedly impaired phosphorylation of DNA-PKcs at Ser2056 in response to IR treatment. Thus, PC3 cells stably expressing a control (shControl) or MEK5 (shMEK5-12) shRNA were exposed to 3 Gy of γ-rays and cells were lysed at different time points (**Figure 4**). Irradiated control PC3 cells showed an increase in phosphorylation of DNA-PKcs at S2056 that peaked 15-30 min post-irradiation, diminishing at later time points. However, PC3 cells with MEK5 knockdown showed a marked reduction in DNA-PKcs activation. In contrast, ATM phosphorylation at S1981 in response to IR was not affected by MEK5. To confirm these results, a different clone of PC3 cells with shMEK5 (#22) (**Figure 5A**), as well as a DU145/shMEK5 clone (#7) (**Figure 5B**) were irradiated. As described for PC3/shMEK5 (#12), DNA-PKcs phosphorylation at S2056 was severely compromised in the MEK5 knocked down cells. Furthermore, ectopic expression of MEK5 in PC3/shMEK5 cells restored activation of DNA-PKcs. Specifically, PC3/shControl, PC3/shMEK5 (#12), or PC3/shMEK5 cells transiently expressing *MEK5* pcDNA3 plasmid were exposed to 3 Gy of γ-rays and cells were lysed at the

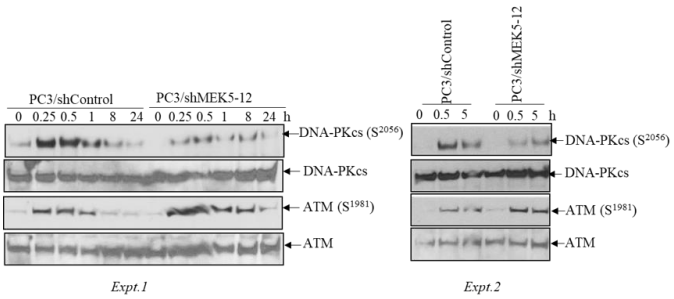


**Figure 4**: **MEK5 knockdown impairs DNA-PKcs phosphorylation.** PC3 cells stable expressing a control (shControl) or MEK5 (shMEK5-12) shRNA were exposed to 3 Gy of γ-rays and cells were lysed at the indicated times. Lysates were separated onto a 3-8% Tris-acetate buffer and immunoblotted sequentially with phospho-DNA-PKcs (Ser2056), total DNA-PKcs, phospho-ATM (Ser1981) and total ATM antibodies. Shown two independent experiments.

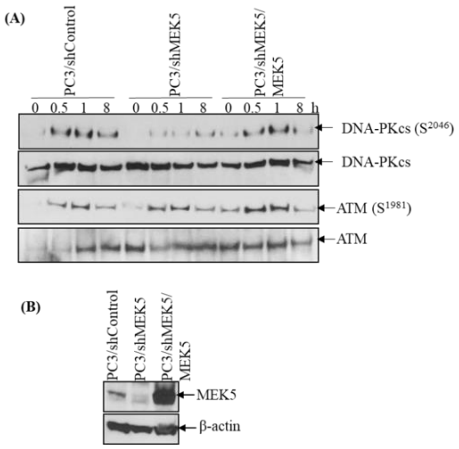


**Figure 6: Ectopic expression of MEK5 restores activation of DNA-PKcs**. **(A)** PC3/shControl, PC3/shMEK5-12, or PC3/shMEK5 cells transiently transfected with a MEK5-pcDNA3 expression vector were exposed to 3 Gy of γ-rays and cells were lysed at the indicated times. Lysates were immunoblotted sequentially with phospho-DNA-PKcs (Ser2056), total DNA-PKcs, phospho-ATM (Ser1981) and total ATM antibodies. **(B)** Protein levels of ectopically expressed MEK5 detected with anti-MEK5 and β-actin (loading control) antibodies.

PC3 cells to etoposide (**Figure 8**).

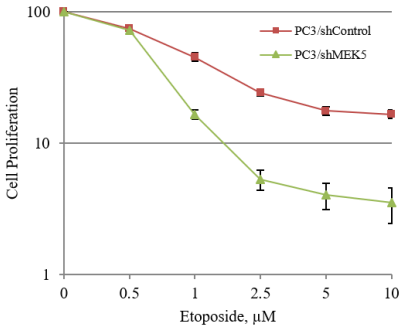


**Figure 8: MEK5 silencing sensitizes cells to etoposide.** PC3 cells were exposed to the indicated doses of etoposide and incubated for 4 days in the presence of the drug, without medium change. Cells were fixed and stained with crystal violet. Color was extracted by acetic acid and absorbance was measured at 595 nm. Data shown are mean ± S. D. (n=3).

indicated times. As shown in **Figure 6A**, while MEK5 knockdown reduced levels of phospho-DNA-PKcs, ectopic expression of MEK5 restored S2056 phosphorylation to normal levels. Finally, similar to stable MEK5 knockdown clones, transient downregulation of MEK5 reduced phospho-DNA-PKcs levels in both PC3 and DU145 cells.

In contrast to castration-resistant prostate cancer cells, MEK5 knockdown did not have an impact on S2056 phosphorylation in response to IR in LNCaP human prostate cancer cell line (**Figure 7A**). A cell growth assay showed that MEK5 downregulation does not sensitize LNCaP cells to IR (**Figure 7B**).

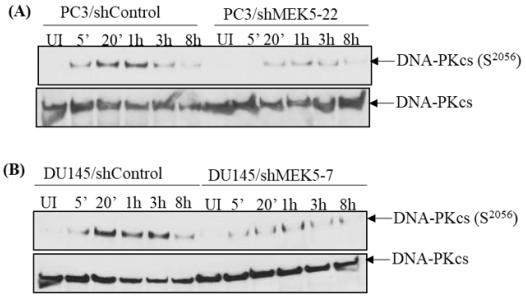


**Figure 5: MEK5 knockdown impairs DNA-PKcs phosphorylation. (A)** PC3 and **(B)** DU145 cells stably expressing a control (shControl) or MEK5 (PC3: shMEK5-22; DU145: shMEK5-7) shRNA were exposed to 3 Gy (PC3) or 4 Gy (DU145) of γ-rays and cells were lysed at the indicated times. Lysates were separated onto a 3-8% Tris-acetate buffer and immunoblotted sequentially with phospho-DNA-PKcs (Ser2056) and total DNA-PKcs antibodies.

Etoposide, a topoisomerase II inhibitor, is a DNA damaging drug that generates double strand breaks. To assess the effect of MEK5 silencing on etoposide-induced stress we performed a dose response experiment. PC3 cells were exposed to various doses of etoposide and incubated for 4 days in the presence of the drug, without medium change. As in the case of IR, MEK5 depletion sensitized

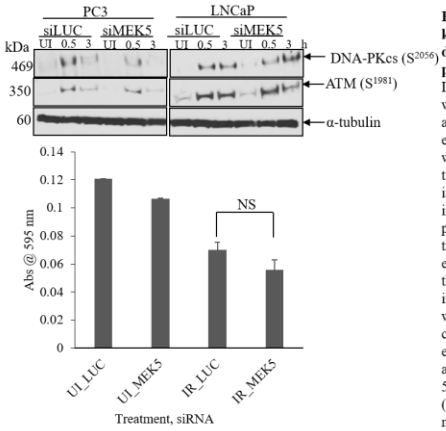


**Figure 7: Transient MEK5 knockdown in LNCaP cells does not impairs DNA-PKcs phosphorylation. (A)** PC3 or LNCaP cells were transfected with siLUC or siMEK5 (#78) and 6 days later they were exposed to 3 Gy γ-rays. Cells were lysed at the indicated times and proteins were immunoblotted with the indicated antibodies. **(B)** Cell proliferation assay. Transiently transfected LNCaP cells were exposed to 3 Gy γ-radiation or they were sham irradiated and incubated for 6 days. Cells were fixed and stained with crystal violet. Color was extracted by acetic acid and absorbance was measured at 595 nm. Data are mean ± S.D. (n=3). UI: unirradiated. NS: not significant.

DNA damage in response to genotoxic stress can be visualized by γH2AX and 53BP1 foci formation, which serve as surrogate markers of DNA double-strand break lesions. Using PC3/shControl and PC3/shMEK5 cells, we showed that MEK5 knockdown did not influence the initial appearance of γH2AX or 53BP1 foci after irradiation, but significantly delayed the resolution of radiation-induced γH2AX and 53BP1 foci, detectable even 48 h post-irradiation (**Figure 9A** and **B**). These results indicate that MEK5 depletion causes a DNA repair defect. Transient MEK5 knockdown in PC3 also showed similar time course resolution of IR-induced DSBs (**Figure 10**). Finally, etoposide treatment produced the same delayed kinetics of 53BP1 foci resolution in PC3/shMEK5 cells compared with PC3/shControl cells (**Figure 11A and B**).

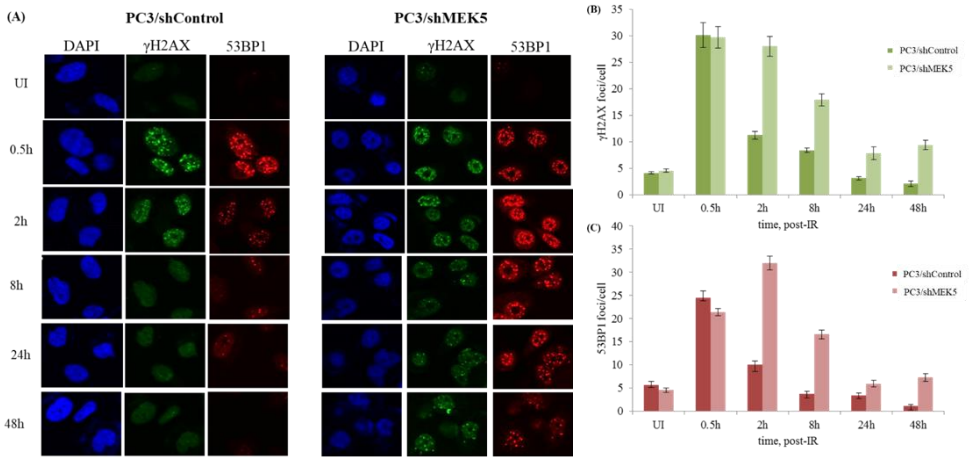


**Figure 9: Stable MEK5 knockdown delays resolution of IR-induced DSBs. (A)** PC3/shControl and PC3/shMEK5 (#12) cells were exposed to 3 Gy of γ-rays and cells were incubated for the indicated times. IR-induced foci were visualized by confocal immunofluorescence. Cells were fixed and stained with anti-γHA2X and anti-53BP1 antibodies and counterstained with DAPI to visualize the nuclei. **(B, C)** Number of foci per cell was automatically counted using the ImageJ software. At least 100 cells in four different fields were enumerated. Data shown are mean ± S. D. (n=3).

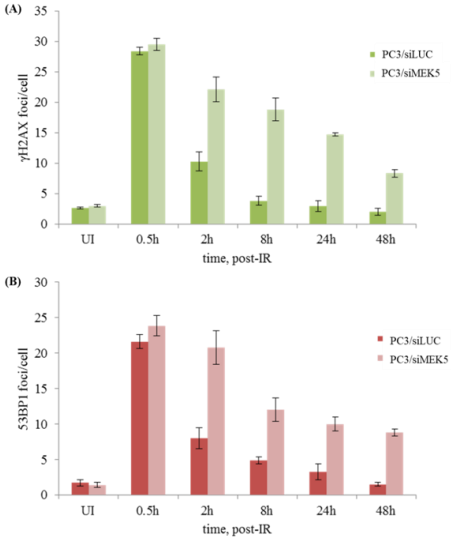


**Figure 10: Transient MEK5 knockdown delays resolution of IR-induced DSBs.** PC3 cells transiently transfected with siMEK5 (#78) or siLuciferase (LUC) and 4 days later, they were exposed to 3 Gy γ-rays and incubated for the indicated time post-irradiation. Cells were fixed and stained using anti-γHA2X **(A)** and anti-53BP1 **(B)** antibodies. Number of foci per cell was automatically counted using the ImageJ software. At least 100 cells in four different fields were enumerated. Data shown are mean ± S. D. (n=3).

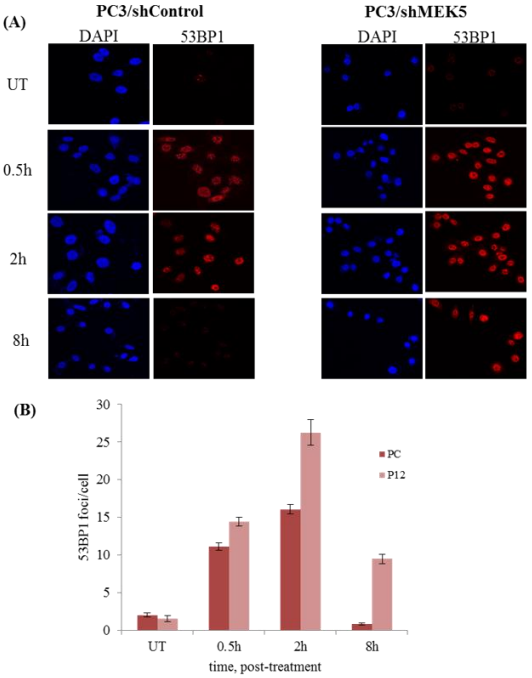


**Figure 11: MEK5 knockdown delays resolution of etoposide-induced DSBs.** PC3/shControl (PC) and PC3/shMEK5 (P12) cells were exposed to 5 μM etoposide overnight, the drug was washed and cells were incubated for the indicated times. Cells were fixed and stained with anti-53BP1 antibodies. **(A)** Etoposide-induced foci were visualized by confocal immunofluorescence. **(B)** Number of foci per cell was automatically counted using the ImageJ software. Data shown are mean ± S. D. (n=3).

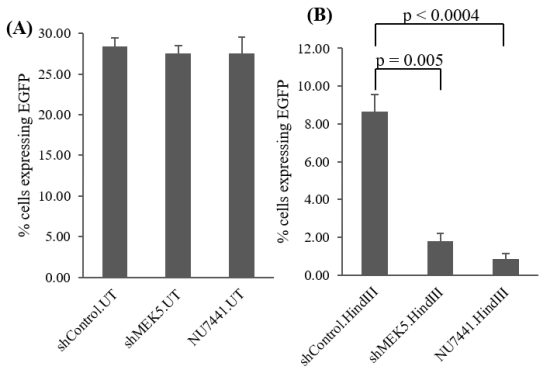


**Figure 12: MEK5 depletion impairs non-homologous end joining**. **(A)** intact or **(B)** HindIII-digested pEGFP-N1 vector was transiently transfected in PC3 cells expressing shControl or shMEK5. shControl cells were also treated or not with NU7441. Twenty-four hours post-transfection, cells were fixed, stained with DAPI, and EGFP-positive cells were quantitated by fluorescence as percent EGFP-positive cells/total (DAPI) number cells. Mean ± S.D. (n = 3). P-value was calculated by Student's t-test. UT: uncut plasmid; HindIII: restriction enzyme-digested plasmid.

DNA-PKcs is a crucial player of the non-homologous end-joining (NHEJ) DNA repair pathway. Thus, we examined the impact of MEK5 deletion on efficiency of NHEJ using a cell-based assay. For this purpose, pEGFP-N1 vector was digested with HindIII restriction endonuclease at a site that lies between the *EGFP* (enhanced green fluorescent protein) gene and its promoter, thus inhibiting *EGFP* transcription. Previously, it had been shown this cut by HindIII is repaired by NHEJ, which then restores *EGFP* transcription, detectable by fluorescence microscopy. pEGFP-N1 plasmid (Clontech) was digested with HindIII restriction endonuclease and transfected into PC3 cells expressing normal or reduced levels of MEK5. As a control, we treated PC3 cells with 2 μM NU7441, a DNA-PKcs-specific inhibitor. Transient transfection efficiency with the initial uncut plasmid was approximately 30% for PC3, PC3/shMEK5, and PC3/NU7441 cells as judged by the number of EGFP fluorescent cells measured under the microscope (**Figure 12A**). Transiently transfected digested plasmid into PC3 cells resulted in approximately 10% of green fluorescent cells that express the protein. In contrast, PC3/shMEK5 produced almost 7 times fewer EGFP-expressing cells (1.5%), whereas the proportion of EGFP-

positive cells after treatment with NU7441 was approximately 1% (**Figure 12B**). Thus, MEK5 downregulation impairs NHEJ.

**Task 3:** Evaluate the efficacy of MEK5 knockdown combined with radiation in the inhibition of prostate tumor growth *in vivo*.

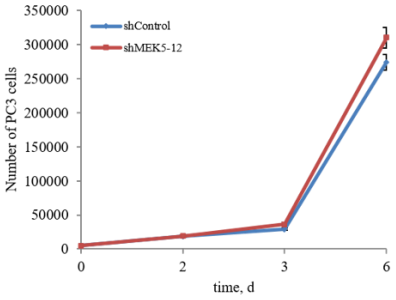


**Figure 13: Cell proliferation**. PC3 (shControl, shMEK5 clone 12) were seeded in 12-well plate (5,000 cells/well). Cells were trypsinized and counted with a hemocytometer at days 0, 2, 3, and 6.

To examine the impact of MEK5 knockdown on the radiosensitization of prostate cancer cells, we used PC3 stably expressing a shRNA targeting MEK5 (clone 12), a clone that shows the greatest MEK5 downregulation, or a non-targeting, control, shRNA. We performed *in vitro* proliferation assays using PC3/shControl and PC3/shMEK5 and demonstrated silencing MEK5 in cells cultured in complete medium (10% fetal bovine serum) grew at similar rates as control PC3 cells (**Figure 13**). Next, we evaluated the efficacy of MEK5 knockdown combined with radiation in the inhibition of prostate tumor growth *in vivo*. All procedures were approved by the Columbia University Institutional Animal Care and Use Committee. Six-week old male athymic NU/J mice (Jackson Laboratory) were injected subcutaneously with $3X10^6$ PC3 cells expressing control (shControl) or MEK5 (shMEK5) shRNA. When tumors reached a volume of approximately ~200 $mm^3$, mice were randomized to one of the following groups: (i) shControl, unirradiated; (ii) shControl; irradiated; (iii) shMEK5; unirradiated; (iv) shMEK5; irradiated. Mice were either left untreated or irradiated with 4 Gy using the Small Animal Radiation Research Platform (SARRP; Xstrahl, Suwanee GA) irradiator as previously described (27). Briefly, mice were anesthetized with 100 mg/kg ketamide and 10 mg/kg xylazine in 0.9% saline by intraperitoneal injection and underwent cone beam computed tomography (CBCT) imaging using the onboard imager of the SARRP for image guided localization of the tumor. A single beam was designed in the sagittal arrangement to deliver 4 Gy radiation through a 10x10 $mm^2$ collimator prescribed to the isocenter.

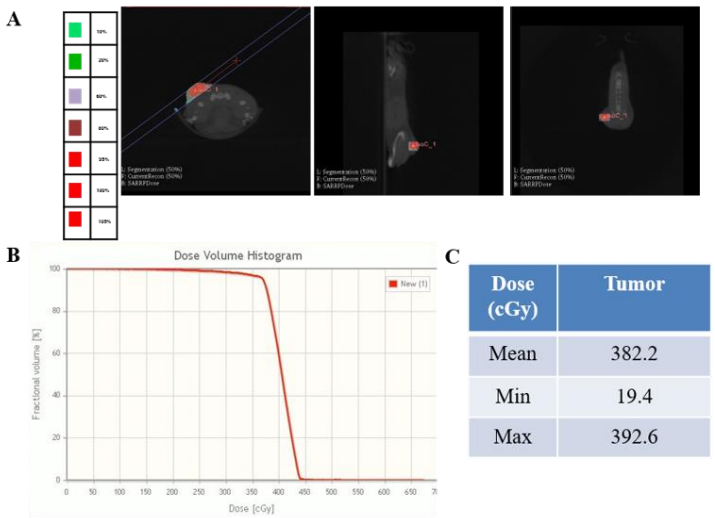


| Dose (cGy) | Tumor |
|---|---|
| Mean | 382.2 |
| Min | 19.4 |
| Max | 392.6 |

**Figure 14: Radiation plan dosimetry and dose-volume histograms.** **(A)** Representative images in coronal, axial and sagittal orientation of tumor-bearing mouse with radiation target volumes (tumor, red; tumor isocenter, cyan) contoured on cone-beam computed tomography images imported into MuriPlan software (Xstrahl, Suwanee, GA). **(B, C)** Representative dose-volume histogram (DVH) and corresponding dosimetry to tumor (mean, minimum and maximum radiation dose (cGy)) for Tumor RT treatment plans.

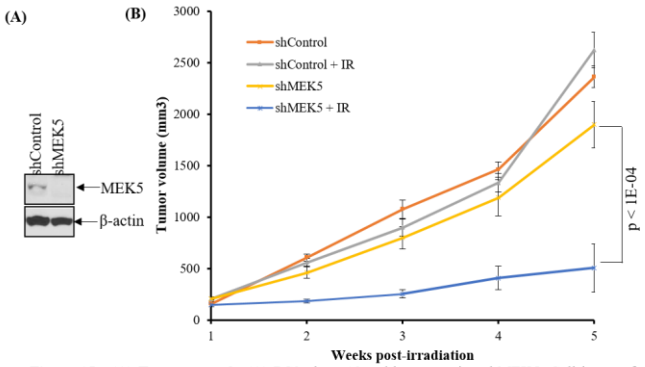


**Figure 15: (A) Tumor growth. (A)** PC3 clone 12 stably expressing shMEK5. Cell lysates from control or clone 12 were immunoblotted with anti-MEK5 and anti-β-actin (loading control) antibodies. **(B)** PC3 cells stably expressing control Scrambled or MEK5 shRNA were injected subcutaneously into athymic male NU/J mice. When tumors reached ~200 $mm^3$, mice were irradiated with 4 Gy x-rays (IR) or they were sham irradiated. Tumor growth was measured using a caliper. Shown mean volume ± S.E.M. (n = 8 mice /treatment).

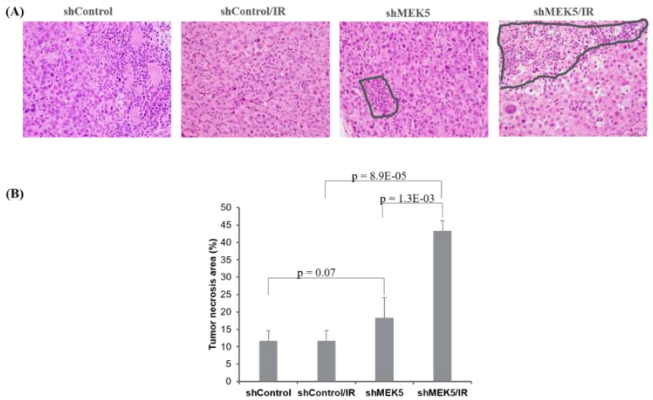


**Figure 16. (A) H & E staining** of PC3 control and MEK5 knockdown tumors with areas of necrosis. Representative FFPE sections from shControl and shMEK5 tumors analyzed by H & E staining. **(B)** Quantitation of necrosis in shControl or shMEK5 tumors exposed or not to irradiation. Mean ± S.E.M. (n = 3).

Radiation was delivered at a potential of 220 kVp and a filament current of 13 mA. Detailed radiation dosimetry and radiation planning information is provided **Figure 14**. Tumor growth was measured twice weekly with a caliper and the volume was estimated according to the formula *Length x Width*$^2$ *x 0.50*, where length is the longest dimension and width the corresponding perpendicular dimension.

PC3/shControl cells were resistant to 4 Gy γ-rays and grew as fast as the control unirradiated cells (**Figure 15**). In contrast, PC3/shMEK5 cells exposed to radiation grew very slowly compared with unirradiated PC3/shMEK5 cells ($p < 4.7E-04$). Finally, Hematoxylin and eosin (H&E) staining revealed that the combination of MEK5 ablation and radiotherapy resulted in extensive tumor necrosis (necrotic areas circled; **Figure 16**).

We conclude that MEK5 knockdown sensitizes PC3 cells to ionizing radiation not only *in vitro*, but also in xenografts.

## Specific Aim 2

**Task 1:** Evaluate the contribution of AKT to MEK5-induced radioresistance by employing both an AKT-specific inhibitor and AKT specific siRNAs in MEK5-expressing cells and expressing an active AKT construct in prostate cancer cells with reduced MEK5 levels: Measure the effect on cell radioresistance by clonogenic survival. Cell lines to be used: DU145, PC3 [ATCC].

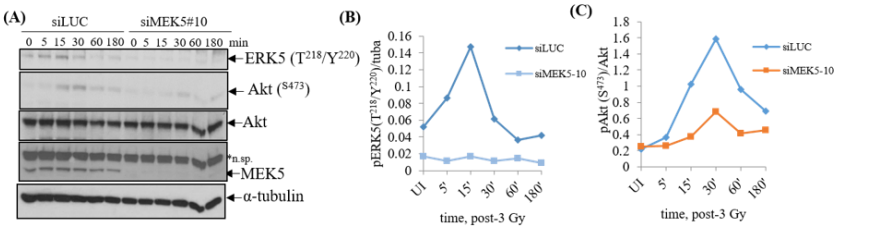


**Figure 17: MEK5 is required for Akt activation after IR. (A)** PC3 cells transiently transfected with either 50 nM siLuc or siMEK5#10 were serum starved for 48h. Cells were irradiated with 3 Gy and lysed at the indicated time points. Levels of phospho-Akt ($S^{473}$), total MEK5 and α-tubulin (loading control) were measured by immunoblotting. **(B)** Quantitation of phospho-ERK5 levels. **(C)** Quantitation of phospho-Akt levels. * n. sp., non-specific.

AKT is phosphorylated in response to DNA damage and downregulation or inhibition of AKT sensitizes cells to IR (28-30). Irradiation of serum-starved PC3 cells leads to $Ser^{473}$ phosphorylation and activation of AKT. Phospho-$Ser^{473}$ increased 15 min post-IR reaching its maximum at 30 min, and then returned to near basal levels by 3 h (**Figure 17**). When MEK5 levels were reduced by siRNA, however, phosphorylation levels of $Ser^{473}$ at its maximal level (30 min) were only ~35% of that of irradiated control PC3 cells (**Figure 17**). We also assessed the impact of MEK5 downregulation on AKT activation in response to IR in DU145 cells. DU145 cells normally express low levels of phospho-AKT. However, when these cells were irradiated, phospho-$Ser^{473}$ levels increased, albeit with slower kinetics than PC3 cells. Thus, AKT phosphorylation peaked at around 8 hr post-IR, while phospho-AKT levels were still detectable 24 h later. As in the case of PC3 cells, MEK5 silencing resulted in reduction in phospho-$Ser^{473}$ abundance in response to 4 Gy γ-rays (**Figure 18**).

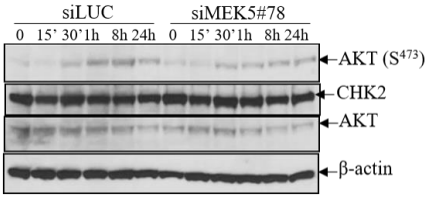


**Figure 18**: **MEK5 depletion impairs AKT activation in irradiated DU145 cells.** Cells were transiently transfected with siLUC or siMEK5 (#78). Four days later, cells were irradiated with 4 Gy γ-rays and lysed at the indicated times. Levels of phospho-Akt ($S^{473}$), total AKT, and α-tubulin (loading control) were measured by immunoblotting.

Combining MEK5 knockdown and AKT activity inhibition by AKT-specific inhibitor MK2206 resulted in less than additive inhibition of cell growth, implying that MEK5 inhibits cell growth in response to IR, at least partially, through AKT (**Figure 19**).

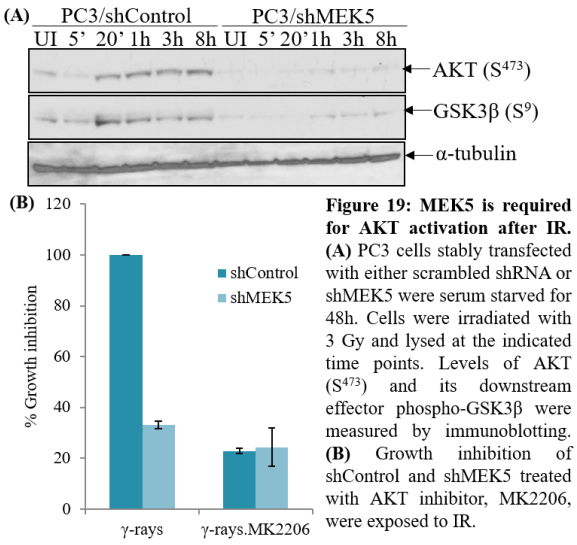


**Figure 19: MEK5 is required for AKT activation after IR. (A)** PC3 cells stably transfected with either scrambled shRNA or shMEK5 were serum starved for 48h. Cells were irradiated with 3 Gy and lysed at the indicated time points. Levels of AKT ($S^{473}$) and its downstream effector phospho-GSK3β were measured by immunoblotting. **(B)** Growth inhibition of shControl and shMEK5 treated with AKT inhibitor, MK2206, were exposed to IR.

**Task 2:** Perform global gene expression analysis.

PC3/shControl and PC3/shMEK5, as well as DU145/shControl and DU145/shMEK5 were exposed to 4 Gy of γ-rays and RNA was isolated 6 h and 24 h post-irradiation. RNA was purified using RNeasy mini kit and RNA yields were quantified using the NanoDrop ND1000 spectrophotometer (Thermofisher) and RNA quality was checked by the 2100 Bioanalyzer (Agilent). High quality RNA with an RNA integrity number of at least 9.0 was used for microarray hybridization. Cyanine-3 labeled cRNA was prepared using the One-Color Low Input Quick Amp Labeling kit (Agilent). Dye incorporation and cRNA yield were measured with a NanoDrop ND1000 spectrophotometer (Thermofisher). Labeled cRNA was fragmented and hybridized to Agilent Human Gene Expression 4x44K v2 Microarray Kit (G4845A). Slides were scanned with the Agilent DNA microarray scanner (G2505B) and the images were analyzed with Feature Extraction software (Agilent) using default parameters for background correction and flagging non-uniform features. There were no radiation-induced genes that were commonly differentially expressed in both PC3 and DU145. However, among unirradiated cells, the two cell lines shared ~15% of the differentially expressed genes. Gene set enrichment analysis (31) revealed that MEK5 ablation in either PC3 or DU145 cells results in the downregulation of genes that are associated with epithelial mesenchymal transition (EMT) (**Figure 20**), a process that has been associated with increased chemo- and radio-resistance (32). Major EMT transcription factors, such as ZEB1, were downregulated in shMEK5-expressing cells (**Figure 20**).

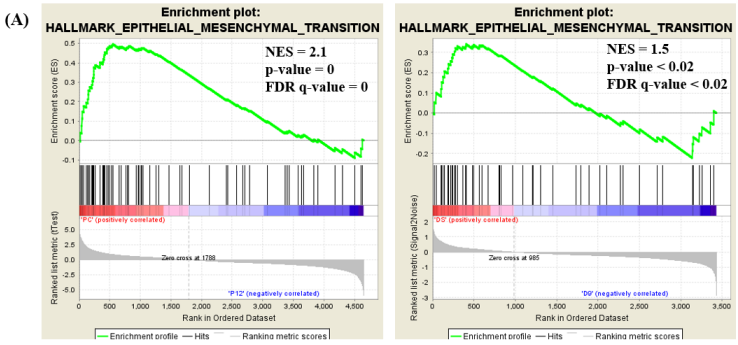


**Figure 20**. **MEK5 is associated with EMT**. **(A)** Gene set enrichment analysis of shControl (PC or DC) and shMEK5 (P12 or D9) gene sets from PC3 and DU145 cells. **(B)** ZEB1 protein levels in PC3 and DU145 cells expressing control (P, D) or MEK5 (clones 12, 22, and 9) shRNA.

## Specific Aim 3

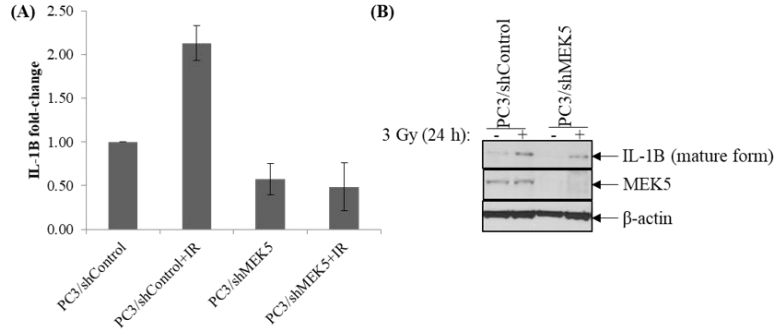


**Figure 21: MEK5 depletion reduces basal and IR-induced IL-1B production.** **(A)** Cells were irradiated with 3 Gy γ-rays and 24 h later, conditioned medium was collected, concentrated and added to antibody arrays. **(B)** Cell were irradiated as in (A) and whole cell lysates were prepared and immunoblotted with anti-IL-1β antibodies, anti-MEK5, and anti-β-actin (loading control).

**Task 1:** Examine the effect of MEK5 on irradiation-induced angiogenesis.

PC3/shControl and PC3/shMEK5 (#12) were exposed to 3 Gy of γ-rays and 24 h later conditioned media was collected. A cytokine antibody array (RayBiotech) revealed that secretion of IL-1β, a known pro-angiogenic factor (33), is increased in the media of control PC3 cells, but not in MEK5-depleted cells (**Figure 21A**). Furthermore, immunoblotting of PC3/shControl cell lysates revealed a similar increase of mature IL-1β protein after irradiation, while IL1β was hardly detectable in PC3/shMEK5 and was increased after irradiation albeit at lower levels compared with irradiated control cells (**Figure 21B**). Further experiments are required to fully elucidate the function of IL-1β in MEK5-induced radioresistance in prostate cancer.

**REFERENCES**


1. Okajima, K, Ishikawa K, Matsuura T, Tatebe H, Fujiwara K, Hiroi K, Hasegawa H, Nishimura Y. (2013). Multiple primary malignancies in patients with prostate cancer: increased risk of secondary malignancies after radiotherapy. Int J Clin Oncol 18(6): 1078-1084. PMID: 23179638.

2. Kuban DA, Tucker SL, Dong L, Starkschall G, Huang EH, Cheung MR, Lee AK, Pollack A. (2008). Long-term results of the M. D. Anderson randomized dose-escalation trial for prostate cancer. Int J Radiat Oncol Biol Phys 70(1): 67-74. PMID: 17765406.

3. Dearnaley DP, Sydes MR, Graham JD, Aird EG, Bottomley D, Cowan RA, Huddart RA, Jose CC, Matthews JH, Millar J, Moore AR, Morgan RC, Russell JM, Scrase CD, Stephens RJ, Syndikus I, Parmar MK; RT01 collaborators. (2007). Escalated-dose versus standard-dose conformal radiotherapy in prostate cancer: first results from the MRC RT01 randomised controlled trial. Lancet Oncol. 8(6):475-87. PMID: 17482880.

4. Zietman AL, DeSilvio ML, Slater JD, Rossi CJ Jr, Miller DW, Adams JA, Shipley WU. (2005). Comparison of conventional-dose vs high-dose conformal radiation therapy in clinically localized adenocarcinoma of the prostate: a randomized controlled trial. JAMA. 294(10):1233-9. PMID: 16160131.

5. Chism DB, Horwitz EM, Hanlon AL, Pinover WH, Mitra RK, Hanks GE. (2003). Late morbidity profiles in prostate cancer patients treated to 79-84 Gy by a simple four-field coplanar beam arrangement. Int J Radiat Oncol Biol Phys. 55(1):71-7. PMID: 12504038.

6. WG, Helle PA, van Putten WL, Wijnmaalen AJ, Seldenrath JJ, van der Werf-Messing BH. (1990). Late radiation damage in prostate cancer patients treated by high dose external radiotherapy in relation to rectal dose. Int J Radiat Oncol Biol Phys. 18(1):23-9. PMID: 2298625.

7. Lawton CA, Won M, Pilepich MV, Asbell SO, Shipley WU, Hanks GE, Cox JD, Perez CA, Sause WT, Doggett SR, et al. (1991). Long-term treatment sequelae following external beam irradiation for adenocarcinoma of the prostate: analysis of RTOG studies 7506 and 7706. Int J Radiat Oncol Biol Phys. 21(4):935-9. PMID: 1917622.

8. Zhou G, Bao ZQ, Dixon JE. (1995). Components of a new human protein kinase signal transduction pathway. J Biol Chem. 270(21):12665-9. PMID: 7759517.

9. Sun W, Kesavan K, Schaefer BC, Garrington TP, Ware M, Johnson NL, Gelfand EW, Johnson GL. (2001). MEKK2 associates with the adapter protein Lad/RIBP and regulates the MEK5-BMK1/ERK5 pathway. J Biol Chem. 276(7):5093-100. PMID: 11073940.

10. Chao TH, Hayashi M, Tapping RI, Kato Y, Lee JD. (1999) MEKK3 directly regulates MEK5 activity as part of the big mitogen-activated protein kinase 1 (BMK1) signaling pathway. J Biol Chem. 274(51):36035-8. PMID: 10593883.

11. Suzaki Y, Yoshizumi M, Kagami S, Koyama AH, Taketani Y, Houchi H, Tsuchiya K, Takeda E, Tamaki T. (2002). Hydrogen peroxide stimulates c-Src-mediated big mitogen-activated protein kinase 1 (BMK1) and the MEF2C signaling pathway in PC12 cells: potential role in cell survival following oxidative insults. J Biol Chem. 277(11):9614-21. PMID: 11782488.

12. Regan CP, Li W, Boucher DM, Spatz S, Su MS, Kuida K. (2002). Erk5 null mice display multiple extraembryonic vascular and embryonic cardiovascular defects. Proc Natl Acad Sci U S A. 99(14):9248-53. PMID: 12093914. PMCID: PMC123126.

13. Yan L, Carr J, Ashby PR, Murry-Tait V, Thompson C, Arthur JS. (2003). Knockout of ERK5 causes multiple defects in placental and embryonic development. BMC Dev Biol. 3:11. PMID: 14675480. PMCID: PMC324396.

14. Wang X, Merritt AJ, Seyfried J, Guo C, Papadakis ES, Finegan KG, Kayahara M, Dixon J, Boot-Handford RP, Cartwright EJ, Mayer U, Tournier C. (2005). Targeted deletion of mek5 causes early embryonic death and defects in the extracellular signal-regulated kinase 5/myocyte enhancer factor 2 cell survival pathway. Mol Cell Biol. 25(1):336-45. PMID: 15601854. PMCID: PMC538774.

15. Sohn SJ, Sarvis BK, Cado D, Winoto A. (2002). ERK5 MAPK regulates embryonic angiogenesis and acts as a hypoxia-sensitive repressor of vascular endothelial growth factor expression. J Biol Chem. 277(45):43344-51. PMID: 12221099.

16. Hayashi M, Fearns C, Eliceiri B, Yang Y, Lee JD. (2005). Big mitogen-activated protein kinase 1/extracellular signal-regulated kinase 5 signaling pathway is essential for tumor-associated angiogenesis. Cancer Res. 65(17):7699-706. PMID: 16140937.

17. Kato Y, Kravchenko VV, Tapping RI, Han J, Ulevitch RJ, Lee JD. (1997). BMK1/ERK5 regulates serum-induced early gene expression through transcription factor MEF2C. EMBO J. 16(23):7054-66. PMID: 9384584. PMCID: PMC1170308.
18. Han TH, Prywes R. (1995). Regulatory role of MEF2D in serum induction of the c-jun promoter. Mol Cell Biol. 15(6):2907-15. PMID: 7760790. PMCID: PMC230521.
19. Pearson G, English JM, White MA, Cobb MH. (2001). ERK5 and ERK2 cooperate to regulate NF-kappaB and cell transformation. J Biol Chem. 276(11):7927-31. PMID: 11118448.
20. Linnerth NM, Baldwin M, Campbell C, Brown M, McGowan H, Moorehead RA. (2005). IGF-II induces CREB phosphorylation and cell survival in human lung cancer cells. Oncogene. 2005 24(49):7310-9. PMID: 16158061.
21. Arnoux V, Nassour M, L'Helgoualc'h A, Hipskind RA, Savagner P. (2008). Erk5 controls Slug expression and keratinocyte activation during wound healing. Mol Biol Cell. 19(11):4738-49. PMID: 18716062. PMCID: PMC2575153.
22. Zhou C, Nitschke AM, Xiong W, Zhang Q, Tang Y, Bloch M, Elliott S, Zhu Y, Bazzone L, Yu D, et al. (2008). Proteomic analysis of tumor necrosis factor-alpha resistant human breast cancer cells reveals a MEK5/Erk5-mediated epithelial-mesenchymal transition phenotype. Breast Cancer Res. 10(6):R105. PMID: 19087274. PMCID: PMC2656902.
23. Schweppe RE, Cheung TH, Ahn NG. (2006). Global gene expression analysis of ERK5 and ERK1/2 signaling reveals a role for HIF-1 in ERK5-mediated responses. J Biol Chem. 281(30):20993-1003. PMID: 16735500.
24. Mehta PB, Jenkins BL, McCarthy L, Thilak L, Robson CN, Neal DE, Leung HY. (2003). MEK5 overexpression is associated with metastatic prostate cancer, and stimulates proliferation, MMP-9 expression and invasion. Oncogene. 22(9):1381-1389. PMID: 12618764.
25. McCracken SR, Ramsay A, Heer R, Mathers ME, Jenkins BL, Edwards J, Robson CN, Marquez R, Cohen P, Leung HY. (2008). Aberrant expression of extracellular signal-regulated kinase 5 in human prostate cancer. Oncogene. 27(21):2978-2988. PMID: 18071319.
26. Ramsay AK, McCracken SR, Soofi M, Fleming J, Yu AX, Ahmad I, Morland R, Machesky L, Nixon C, Edwards DR, Nuttall RK, Seywright M, Marquez R, Keller E, Leung HY. (2011). ERK5 signalling in prostate cancer promotes an invasive phenotype. Br J Cancer. 104(4):664-72. PMID: 21266977. PMCID: PMC3049582.
27. Wu CC, Chaudhary KR, Na YH, Welch D, Black PJ, Sonabend AM, Canoll P, Saenger YM, Wang TJC, Wuu CS, Hei TK, Cheng SK. Quality Assessment of Stereotactic Radiosurgery of a Melanoma Brain Metastases Model Using a Mouselike Phantom and the Small Animal Radiation Research Platform. Int J Radiat Oncol Biol Phys. 2017;99(1):191-201. PMID: 28816146 PMCID: PMC5675116.
28. Toulany M, Kehlbach R, Florczak U, Sak A, Wang S, Chen J, Lobrich M, Rodemann HP. (2008). Targeting of AKT1 enhances radiation toxicity of human tumor cells by inhibiting DNA-PKcs-dependent DNA double-strand break repair. Mol Cancer Ther. 7(7):1772-1781. PMID: 18644989.
29. Fraser M, Harding SM, Zhao H, Coackley C, Durocher D, Bristow RG. (2011). MRE11 promotes AKT phosphorylation in direct response to DNA double-strand breaks. Cell Cycle. 10(13):2218-2232. PMID: 21623170.
30. Kim IA, Bae SS, Fernandes A, Wu J, Muschel RJ, McKenna WG, Birnbaum MJ, Bernhard EJ. (2005). Selective inhibition of Ras, phosphoinositide 3 kinase, and Akt isoforms increases the radiosensitivity of human carcinoma cell lines. Cancer Res. 65(17):7902-7910. PMID: 16140961.
31. Subramanian A, Tamayo P, Mootha VK, Mukherjee S, Ebert BL, Gillette MA, Paulovich A, Pomeroy SL, Golub TR, Lander ES, Mesirov JP. Gene set enrichment analysis: a knowledge-based approach for interpreting genome-wide expression profiles. Proc Natl Acad Sci U S A. 2005;102(43):15545-50. PMID: 16199517 PMCID: PMC1239896.
32. Chang L, Graham PH, Hao J, Bucci J, Cozzi PJ, Kearsley JH, Li Y. Emerging roles of radioresistance in prostate cancer metastasis and radiation therapy. Cancer Metastasis Rev. 2014;33(2-3):469-96. PMID: 24445654.
33. Voronov E, Shouval DS, Krelin Y, Cagnano E, Benharroch D, Iwakura Y, Dinarello CA, Apte RN. (2003) IL-1 is required for tumor invasiveness and angiogenesis. Proc Natl Acad Sci U S A. 100(5):2645-50. PMID: 12598651.

**What opportunities for training and professional development has the project provided?**
Nothing to Report

**How were the results disseminated to communities of interest?**
(1) Oral and poster presentations. Details in *Products* section and *Appendix 1*.
(2) Peer-reviewed publication. Details in *Products* section.

**What opportunities for training and professional development has the project provided?**
Nothing to Report

**What do you plan to do during the next reporting period to accomplish the goals?**
Project has been completed

**What was the impact on the development of the principal discipline(s) of the project?**
We have discovered that MEK5 downregulation sensitizes prostate cancer cells to radiotherapy. Mechanistically, MEK5 knockdown leads to reduced phosphorylation/activation of DNA-PKcs, delays repair of DNA double strand breaks, as judged by the persistence of γH2AX and 53BP1 IR-induced foci and impairs non-homologous-end joining. Finally, our *in vivo* experiments confirm the importance of MEK5 silencing as a radiosensitizing modality.

**What was the impact on other disciplines?**
Nothing to Report

**What was the impact on technology transfer?**
Nothing to Report

**What was the impact on society beyond science and technology?**
Nothing to Report

**CHANGES/PROBLEMS**

**Changes in approach and reasons for change**
Nothing to report

**Actual or anticipated problems or delays and actions or plans to resolve them**
Angiogenesis experiments using Human Prostate Microvascular Endothelial Cells from a commercial source were not feasible, because cells acquired a senescent phenotype soon after culturing them *in vitro* and therefore they could not be propagated in culture for functional assays.

**Changes that had a significant impact on expenditures**
Nothing to Report

**Significant changes in use or care of human subjects, vertebrate animals, biohazards, and/or select agents**
No change

## PRODUCTS

### Publications, conference papers, and presentations

**Publication**
Broustas CG, Duval AJ, Chaudhary KR, Friedman RA, Virk RK, Lieberman HB. Targeting MEK5 impairs non-homologous end-joining repair and sensitizes prostate cancer to DNA damaging agents. Oncogene. 2020 (*In press*).

**Conference Paper**
Constantinos G. Broustas. MEK5 downregulation enhances radiosensitization of human prostate cancer cells by inhibiting DNA repair [abstract]. In: Proceedings of the AACR Special Conference: Prostate Cancer: Advances in Basic, Translational, and Clinical Research; 2017 Dec 2-5; Orlando, Florida. Philadelphia (PA): AACR; Cancer Res 2018;78(16 Suppl):Abstract nr B030.
http://cancerres.aacrjournals.org/content/78/16_Supplement/B030

**Conference Paper**
Constantinos G. Broustas. Downregulation of MEK5 Sensitizes Human Prostate Cancer Cells to Ionizing Radiation. Abstract *in* PCRP - Innovative Minds in Prostate Cancer Today (IMPaCT), Towson, MD. August 4-5, 2016.

**Presentation**
Broustas, CG. "Targeting MEK5 sensitizes prostate cancer cells to genotoxic stress". Radiation Oncology Research Retreat, Columbia University Medical Center, October 6th, 2017.

Broustas, CG. "Role of MEK5 in radiosensitivity of prostate cancer cells". Radiation Oncology Research Retreat, Columbia University Medical Center, November 15th, 2019.

## PARTICIPANTS AND OTHER COLLABORATING ORGANIZATIONS

**What individuals have worked on the project?**
Name: Constantinos G. Broustas
Project Role: PI
Nearest Person month worked: 5
Contribution to Project: Designed, performed, interpreted experiments

Name: Richard A. Friedman
Project Role: co-I
Nearest Person month worked: 0.5
Contribution to Project: Performed statistical analyses

**Has there been a change in the active other support of the PD/PI(s) or senior/key personnel since the last reporting period?**
Nothing to Report

**What other organizations were involved as partners?**
Nothing to Report

## SPECIAL REPORTING REQUIREMENTS
Nothing to Report

**APPENDICES**

1

**APPENDIX**

**Conference Paper**

Constantinos G. Broustas. MEK5 downregulation enhances radiosensitization of human prostate cancer cells by inhibiting DNA repair [abstract]. In: Proceedings of the AACR Special Conference: Prostate Cancer: Advances in Basic, Translational, and Clinical Research; 2017 Dec 2-5; Orlando, Florida. Philadelphia (PA): AACR; Cancer Res 2018;78(16 Suppl):Abstract nr B030.
http://cancerres.aacrjournals.org/content/78/16_Supplement/B030

Radiotherapy is commonly used to treat a variety of solid human tumors, including localized prostate cancer. However, treatment failure almost always ensues due to tumor intrinsic or acquired radioresistance.
Mitogen-activated protein kinase kinase 5 (MAP2K5 or MEK5), belongs to the family of MAP kinases. It is activated by the upstream kinases MEKK2 and MEKK3 at Ser311/Thr315. MEK5, in turn, phosphorylates and activates extracellular signal-regulated kinase 5 (ERK5 or BMK1) at Thr218/Tyr220. MEK5/ERK5 pathway plays a pivotal role in tumor initiation and progression. MEK5 protein is overexpressed in prostate cancer cells compared with normal prostate epithelial cells, and MEK5 levels are correlated with prostate cancer metastasis. High expression of ERK5 in prostate cancer is also found to correlate with poor disease-specific survival and can serve as an independent prognostic factor.
To determine whether the MEK5/ERK5 pathway is activated in response to ionizing radiation (IR), RNA interference was used to deplete MEK5 from PC3 and DU145 cells. Western blot analysis demonstrated that control cells with normal levels of MEK5 exposed to 3-Gy γ-rays had an increase in phospho-ERK5 levels at 5 and 15 min post-IR, diminishing at later time points. No activated ERK5 was detected in MEK5-depleted cells. Downregulation of MEK5 did not impact on cell cycle checkpoint activation in irradiated cells. In contrast, depletion of MEK5 markedly impaired phosphorylation of DNA-PKcs at Ser2056 in response to IR treatment. Furthermore, MEK5 knockdown did not influence the initial appearance of γH2AX or 53BP1 foci after irradiation, but significantly delayed the resolution of radiation-induced γH2AX and 53BP1 foci, detectable even 48 h post-irradiation, indicating a DNA repair defect. Cell based assay showed that nonhomologous end-joining is compromised in PC3 cells with ablated MEK5 protein expression. Finally, long-term clonogenic survival analyses and short-term cell growth assays indicated that MEK5 knockdown sensitized PC3 and DU145 prostate cancer cell lines to IR. Likewise, the topoisomerase II inhibitor etoposide that causes double-strand breaks also sensitized MEK5-depleted cells.
These data indicate that MEK5 influences the response of prostate cancer cells to radiation and MEK5 downregulation is associated with delayed double-strand break repair kinetics. Inhibition of MEK5 in combination with radiation may provide a strategy to improve survival of prostate cancer patients.

**Conference Paper**

Constantinos G. Broustas. Downregulation of MEK5 Sensitizes Human Prostate Cancer Cells to Ionizing Radiation. Abstract *in* PCRP - Innovative Minds in Prostate Cancer Today (IMPaCT), Towson, MD. August 4-5, 2016.
**Background & Objectives:** Tumor cell resistance to ionizing radiation (IR) poses a major obstacle in prostate cancer therapy. Mitogen/extracellular signal-regulated kinase kinase-5 (MEK5) belongs to the family of MAP kinases. It is activated by the upstream kinases MEKK2 and MEKK3. MEK5, in turn, phosphorylates and activates extracellular signal-regulated kinase 5 (ERK5) at Thr218/Tyr220. MEK5/ERK5 pathway plays a pivotal role in tumor initiation and progression, including prostate cancer. MEK5 protein is overexpressed in prostate cancer cells compared with normal cells and MEK5 levels are correlated with prostate cancer metastasis. This study explores the hypothesis that MEK5 is a contributing factor to the response of prostate cancer cells to IR and seeks to elucidate the mechanism by which MEK5 affects radioresistance.

**Methods:** Castration-resistant DU145, PC3, and PC3MM2, as well as androgen-dependent LNCaP prostate cancer cells were treated with MEK5 short interfering (si) RNA alone or in combination with γ-rays. Clonogenic survival assays, cell cycle analysis, immunofluorescence and immunoblotting were performed to assess cell proliferation, survival, cell cycle progression and DNA damage response.
**Results:** We examined MEK5/ERK5 pathway activation in response to IR in prostate cancer cells transiently expressing *Luciferase* (control) or *MEK5* siRNAs. Control cells with normal levels of MEK5 showed an increase in phospho-ERK5 levels at 5 and 15 min post-IR, diminishing at later time points. In addition, we discovered that AKT activation after 4 Gy IR was dependent on the presence of MEK5. AKT phosphorylation at Ser473, which is considered a marker of AKT activation, was increased reaching maximal levels at 30 min post-IR. In contrast, when MEK5 was downregulated by MEK5 specific siRNAs, AKT activation was severely impaired. Moreover, MEK5 silencing had an impact on the DNA damage response pathway. Specifically, MEK5 knockdown, combined with IR, resulted in significantly higher phospho-CHK2 (Thr68) levels 30 min after irradiation compared with irradiated cells with endogenous levels of MEK5. Additionally, increased levels of phospho-CHK2 persisted for at least 8 h post-irradiation, whereas the phospho-CHK2 signal returned to near basal levels by 3 h in control cells. On the other hand, CHK1 phosphorylation at Ser345 and activation in response to IR was elevated in MEK5 control cells 30 min post-irradiation compared with MEK5 knockdown cells. Finally, MEK5 depletion by two non-overlapping siRNAs sensitized prostate cancer cells to IR as determined by clonogenic survival assay. Short-term targeting of MEK5 in combination with IR led to approximately 70% reduction in prostate cancer cell proliferation 6 days post-irradiation.
**Conclusions:** These data indicate that MEK5 knockdown radiosensitize prostate cancer cells. In response to IR, MEK5 controls activation of AKT, a kinase involved in radioresistance, as well as DNA damage response by regulating activation of CHK1/2 kinases. Ongoing studies focus on determining the contribution of AKT and CHK1/2 kinases and their downstream effectors to MEK5-dependent radioresistance.
**Impact**: This study focuses on mechanisms of resistance to radiotherapy for patients with localized prostate cancer. Downregulation of MEK5 can selectively radiosensitize prostate tumors, while sparing normal tissue, thus improving survival of cancer patients.

**Accepted Manuscript for Publication**

# Targeting MEK5 impairs non-homologous end-joining repair and sensitizes prostate cancer to DNA damaging agents

Constantinos G. Broustas[1*], Axel J. Duval[1], Kunal R. Chaudhary[1], Richard A. Friedman[2], Renu K. Virk[3], and Howard B. Lieberman[1,4]

[1]Center for Radiological Research, Columbia University Vagelos College of Physicians and Surgeons, Columbia University Irving Medical Center, New York, NY, USA

[2]Biomedical Informatics Shared Resource, Herbert Irving Comprehensive Cancer Center and Department of Biomedical Informatics, Columbia University Irving Medical Center, New York, NY, USA

[3]Department of Pathology and Cell Biology, Columbia University Irving Medical Center, New York, NY, USA

[4]Department of Environmental Health Sciences, Mailman School of Public Health, Columbia University, New York, NY, USA

*Correspondence should be addressed to: Dr. Constantinos G. Broustas, Center for Radiological Research, Columbia University Vagelos College of Physicians and Surgeons, 630 W. 168th St., New York, NY 10032; E-mail: cgb2117@cumc.columbia.edu.

Running Title: MEK5 silencing sensitizes human prostate cancer to DNA damage.

**Abstract**

Radiotherapy is commonly used to treat a variety of solid human tumors, including localized prostate cancer. However, treatment failure often ensues due to tumor intrinsic or acquired radioresistance. Here we find that the MEK5/ERK5 signaling pathway is associated with resistance to genotoxic stress in aggressive prostate cancer cells. MEK5 knockdown by RNA interference sensitizes prostate cancer cells to ionizing radiation (IR) and etoposide treatment, as assessed by clonogenic survival and short-term proliferation assays. Mechanistically, MEK5 downregulation impairs phosphorylation of the catalytic subunit of DNA-PK at serine 2056 in response to IR or etoposide treatment. Although MEK5 knockdown does not influence the initial appearance of radiation- and etoposide-induced γH2AX and 53BP1 foci, it markedly delays their resolution, indicating a DNA repair defect. A cell-based assay shows that non-homologous end joining (NHEJ) is compromised in cells with ablated MEK5 protein expression. Finally, MEK5 silencing combined with focal irradiation causes strong inhibition of tumor growth in mouse xenografts, compared with MEK5 depletion or radiation alone. These findings reveal a convergence between MEK5 signaling and DNA repair by NHEJ in conferring resistance to genotoxic stress in advanced prostate cancer and suggest targeting MEK5 as an effective therapeutic intervention in the management of this disease.

**Introduction**

Radiotherapy is a common therapeutic modality for the treatment of human epithelial tumors, including those of prostate origin [1]. Despite considerable improvements in delivering the radiation dose with precision, therapeutic benefit in prostate cancer radiotherapy has been hampered by tumor resistance to ionizing radiation. Tumor-intrinsic pro-survival pathways, as well as upregulation of DNA repair pathways constitute major mechanisms by which malignant cells become radioresistant [2].

Cells react to genotoxic insults by engaging a highly intricate DNA damage response and repair network, which is mediated by the phosphoinositide-3-kinase-like kinases (PIKKs) DNA-PK (DNA-dependent protein kinase), ATM (ataxia telangiectasia mutated), and ATR (ATM and Rad3-related) [3]. DNA-PK and ATM are activated

by DSBs, whereas ATR plays a leading role in response to DNA single-strand breaks [3]. DNA double strand breaks (DSBs) induced by ionizing radiation or certain chemotherapeutic agents potentially represent a highly toxic form of DNA damage that leads to cell death or genomic instability. In mammals, there are two major pathways for repairing DSBs. Homologous recombination (HR) is predominantly error-free repair and active during the S and G2 phases of the cell cycle, and non-homologous end-joining (NHEJ) that can be either error-free or error-prone and is active throughout the cell cycle [4, 5]. NHEJ is the dominant pathway for repairing DNA DSBs in mammalian somatic cells [6]. Central to NHEJ repair is the DNA-PK trimeric complex, composed of DNA-PK catalytic subunit (DNA-PKcs) and DNA binding subunits, KU70 and KU80. Both KU70 and KU80 bind to DNA breaks and activate DNA-PKcs kinase activity to initiate DNA repair by NHEJ [7]. Phosphorylation at Threonine 2609 (S2609) and Serine 2056 (S2056) in response to DNA DSBs is associated with repair efficiency of DNA-PKcs [8].

Mitogen-activated protein kinase kinase 5 (MAP2K5 or MEK5) belongs to the family of MAP kinases. It is activated by the upstream kinases MEKK2 and MEKK3 at serine 311 and threonine 315 (S311/T315), or in some cases directly by c-Src [9-12]. MEK5, in turn, phosphorylates and activates extracellular signal-regulated kinase 5 (ERK5 or BMK1) at T218/Y220 [9]. The MEK5/ERK5 pathway can be activated by various stimuli such as oxidative stress, growth factors, and mitogens downstream of receptor tyrosine kinases, as well as G protein-coupled receptors, and culminates in the activation of a large number of transcription factors, including MEF2 (myocyte enhancer factor 2), c-JUN, NF-κB, and transcription factors that control the epithelial-mesenchymal transition (EMT) program [13-18]. Furthermore, recent reports have shown that ERK5 is activated by oncogenic BRAF and promotes melanoma growth [19], whereas inhibition of ERK1/2 in melanoma leads to compensatory activation of the MEK5/ERK5 pathway [20].

The MEK5/ERK5 pathway plays a pivotal role in prostate cancer initiation and progression. MEK5 protein is overexpressed in prostate cancer cells compared with normal cells and MEK5 levels are correlated with prostate cancer metastasis [21]. Furthermore, high expression of ERK5 in prostate cancer has also been found to correlate with poor disease-specific survival and could serve as an independent prognostic factor [22]. Moreover, ERK5

expression in prostate cancer is associated with an invasive phenotype [23]. Recently, it has been shown that deletion of *Erk5* in an established *Pten*-deficient mouse model of human prostate cancer can increase T-cell infiltration and control tumor growth [24].

The present study was designed to investigate whether MEK5 downregulation sensitizes human prostate cancer cells to radiation and other agents that inflict DNA DSBs, and examine the potential mechanism of sensitization to these drugs. We show that MEK5 knockdown enhances the sensitivity of human prostate cancer cells to radiation and etoposide, which, mechanistically, can be attributed to inhibition of DNA-PKcs phosphorylation and the non-homologous end-joining process. Importantly, *in vivo* studies using a mouse xenograft model show that MEK5 ablation synergizes with radiation to suppress tumor growth. Our results support the hypothesis that inactivation of MEK5 in prostate cancer could be a strategy for improving the efficacy of radiotherapy in prostate cancer patients.

## Results

### MEK5/ERK5 pathway activation in response to ionizing radiation

It has been demonstrated previously that MEK5 and ERK5 are upregulated in human prostate cancer and are associated with metastasis and reduced patient survival [25-27]. Immunoblotting of a panel of normal and malignant human prostate cell lines showed that MEK5 is predominantly expressed in advanced prostate cancer cell lines PC3 and DU145, less in androgen-responsive LNCaP, and at very low levels in normal epithelial prostate cells (PrEC) and the immortalized, but non-tumorigenic, cell line EP156T (Supplementary Fig. 1).

The MEK5/ERK5 pathway is activated by a diverse array of growth factor, cytokines, as well as stress in the form of osmotic stress. We sought to determine whether the MEK5/ERK5 pathway is activated in response to ionizing radiation (IR) in human prostate cancer. Using phospho-ERK5 (T218/Y220) levels as a readout for the activation of the pathway, we exposed DU145 expressing either *MEK5* or control *Luciferase* siRNA to different doses of IR and lysed the cells 15 min post-irradiation. As shown in Fig. 1a, phospho-ERK5 levels were increased after 2 and 4 Gy of γ-rays. We repeated the experiment by exposing PC3 cells to 3 Gy of IR and lysing the cells at various

times post-irradiation. Activation of ERK5 in response to IR was fast occurring already at the earliest examined time (5 min) and persisting up to 15-30 min, gradually diminishing at later time points (Fig. 1b). As expected no phospho-ERK5 was detected in the MEK5 depleted DU145 of PC3 cells. Similarly, PC3 cells stably expressing *MEK5* shRNA had reduced levels of activated ERK5, while control cells, stably expressing a scrambled shRNA, showed increase in phospho-ERK5 (T218/Y220) at 10 min post-irradiation that returned to basal levels by 4 h (Fig. 1c). We conclude that ionizing radiation induces a fast and transient activation of MEK5/ERK5 signaling pathway.

**Clonogenic survival assay**

To assess the physiological significance of IR-induced MEK5/ERK5 pathway activation, we next assessed the ability of MEK5 depletion to radiosensitize human prostate cancer cells using clonogenic survival assays. For this purpose, we transiently depleted MEK5 from DU145 (four non-overlapping siRNA against MEK5) or PC3 (two independent siMEK5) and two days later irradiated cells with a range of γ-rays. siRNA treatment was able to suppress MEK5 protein levels for at least 7 days (Supplementary Fig. 2a, b). The number of radioresistant clones was recorded in control cells (transfected with *Luciferase* siRNA) and compared with MEK5-depleted cells. *MEK5* knockdown led to significant reproductive cell death after irradiation compared with irradiated cells transfected with *Luciferase* siRNA (Fig. 1d, e). Specifically, knocking down MEK5 by each of four non-overlapping siRNAs sensitized DU145 cells to radiation (surviving fraction at 2 Gy [$SF_2$] 0.54 ± 0.02) compared to either parental cells or cells transfected with control luciferase siRNA ($SF_2$ 0.78 ± 0.05) (Fig. 1d). Similar radiosensitization was achieved with PC3 cells ($SF_2$ 0.35 ± 0.04 vs. 0.20 ± 0.03 in control vs. siMEK5) (Fig. 1e). We also performed shorter-term cell proliferation assays with PC3 and DU145 cells transiently expressing *MEK5* or *Luciferase* siRNA irradiated or not with 4 Gy, and cells were counted 6 days later. Transfection of untreated PC3 or DU145 cells with siMEK5 did not affect cell proliferation, appreciably. However, cells with MEK5 knockdown showed marked radiosensitization. Thus, cell proliferation of irradiated DU145 cells expressing control siRNA was reduced to 65.1 ± 1.7% (n = 3), whereas in MEK5 knockdown DU145 cells proliferation was

28.2 ± 2.9% (n = 3; p < 0.005), compared with unirradiated control cells. Likewise, proliferation of irradiated PC3 cells expressing *Luciferase* or *MEK5* siRNA were 38.3 ± 4.1% (n = 3) and 13.9 ± 2.3% (n = 3) (p < 0.004), respectively (Fig. 1f). Next, we established PC3 and DU145 cells stably expressing *MEK5* or scrambled (shControl) shRNA and isolated 2 clones (#12, #22) for PC3 and 3 clones (denoted #5, #7, and #9) for DU145 cells that showed downregulation of endogenous MEK5 protein (Supplementary Fig. 2c, d). We exposed DU145/shMEK5#9 cells and PC3/shMEK5#12 to 4 Gy (DU145) or 3 Gy (PC3) of γ-rays. In agreement with the clonogenic assay results, silencing of *MEK5* resulted in significant radiosensitization in both DU145 (30.8 ± 2.1%; n = 3; p = 2.9E-06) and PC3 (15.7 ± 0.4%; n = 3; p = 6.4E-05) cells 6 days post-irradiation compared with shControl cells (Fig. 1g and Supplementary Fig. 3 for an additional independent experiment).

**Cell cycle checkpoint activation in response to IR is not affected by MEK5**

Cells exposed to genotoxic stress, such as IR, arrest the cell cycle at various phases and attempt to repair the DNA damage. In particular, cells that lack a functional p53, such as PC3 and DU145, arrest the cell cycle at G2/M phase. To determine the impact of MEK5 knockdown on cell cycle checkpoint activation after irradiation we analyzed cell cycle distribution. As expected, irradiation of either DU145 or PC3 cells caused a G2/M arrest starting at about 8 h post-IR, whereas by 48 h cells had resumed their normal cell cycle activity. However, transient or stable downregulation of MEK5 did not appreciably affect cell cycle distribution after irradiation (Supplementary Fig. 4a, b). These results suggest that MEK5 does not play a role in enforcing cell cycle checkpoint activation in response to IR.

**DNA-PKcs activation in response to genotoxic stress is compromised in MEK5 knockdown cells**

Many studies have linked defects in DNA repair mechanisms to enhanced radiosensitivity. DNA double strand breaks inflicted by ionizing radiation, etoposide, and other anticancer agents lead to activation of kinases ATM and DNA-PKcs that initiate DNA repair. Activation of ATM is primarily monitored by phosphorylation of serine 1981 (S1981) and ATM is pivotal in the activation of DNA repair by homologous recombination. DNA-PKcs

contains multiple Ser/Thr phosphorylation sites, and its DNA damage-inducible autophosphorylation site at S2056 is required for the repair of double-strand breaks by NHEJ [8]. Phosphorylation of serine 2056 (S2056), along with phosphorylation at threonine 2609 (T2609), are considered markers for DNA-PKcs activation in response to DNA damage [7]. Thus, to investigate the potential molecular mechanisms underlying the enhanced sensitivity of MEK5 knockdown in prostate cancer cells to IR, we examined phosphorylation status of DNA-PKcs and ATM in response to DNA damage. PC3 cells transiently expressing a control *Luciferase* siRNA (siLUC) responded to 3 Gy γ-rays by a robust increase in phosphorylation of DNA-PKcs at S2056 and T2609 that was detectable at the earliest time point examined (15 min) post-irradiation. DNA-PKcs phosphorylation signal was diminished to near basal levels 3 h post-irradiation, suggesting completion of DNA repair [7]. In contrast, DNA-PKcs phosphorylation was severely diminished in MEK5 depleted PC3 cells (Fig. 2a). On the other hand, ATM phosphorylation at S1981 in response to IR was comparable between control and MEK5-depleted PC3 cells (Fig. 2a). These results were also confirmed by using DU145 cells (Fig. 2b). We also examined phosphorylation of DNA-PKcs at S2056 using PC3 cells stably expressing MEK5 shRNA (clones #12, #22) or control shRNA (shControl) (Fig. 2c and Supplementary Fig. 5), as well as DU145 cells expressing MEK5 shRNA (clone #7) (Fig. 2d) with similar results. Finally, ectopic expression of a MEK5 construct (Supplementary Fig. 1e) in PC3/shMEK5 (clone #12) cells showed that DNA-PKcs S2056 phosphorylation was restored to normal levels in response to irradiation, while phospho-ATM remained at similar levels between shMEK5 and shMEK5/MEK5 cells (Fig. 2e).

We also examined the impact of MEK5 silencing on the response to IR of two additional cell lines, the non-tumorigenic prostate epithelial cells EP156T and the androgen-responsive LNCaP cells. In contrast to PC3 and DU145, MEK5 ablation did not have an impact on the phosphorylation of DNA-PKcs (S2056) and ATM (S1981) in response to IR (Supplementary Fig. 6a, b). Likewise, cell proliferation assay showed that MEK5 ablation did not sensitize LNCaP cells to IR (Supplementary Fig. 6c).

To validate the impact of MEK5 silencing on DNA-PKcs activation further, we exposed PC3 and DU145 cells to etoposide and phleomycin, two compounds that inflict cell damage by generating DNA double strand breaks,

which are predominantly repaired by NHEJ [28]. We first performed a dose response study using various concentrations (0, 0.5, 1, 2.5, 5, and 10 μM) of etoposide with PC3/shControl and PC3/shMEK5-12 cells. As shown in Fig. 3a, PC3 cells with MEK5 knockdown were exquisitely sensitive to etoposide treatment compared with control PC3 cells. In a similar experiment, we treated PC3/shControl and PC3/shMEK5-12 cells with 10 μM etoposide for 16 h, removed the drug, and incubated cells for an additional 4 days after which we counted the cells. While total cell count of untreated PC3 expressing shMEK5 did not differ from control cells, etoposide-exposed PC3/shMEK5 showed an 80% reduction in cell numbers compared with etoposide-treated control cells (Fig. 3b). Furthermore, treating PC3 cells with 10 μM of etoposide resulted in a robust increase of DNA-PKcs phosphorylation at S2056 (Fig. 3c). In contrast, phospho-DNA-PKcs was significantly lower in PC3/shMEK5 cells for the whole time course (Fig 3c and Supplementary Fig. 7a). These results were further confirmed with DU145 cells, as well (Supplementary Fig. 7b). ATM activation was not different between control and *MEK5* knockdown PC3 cells. Finally, we treated PC3 and DU145 cells with 60 μg/mL of phleomycin for 2 h to generate DSBs, removed the drug, and incubated the cells in drug-free culture medium for up to 4 h. As seen with IR and etoposide, the expected increase in phospho-S2056 was observed only in the cells with normal levels of MEK5, but not in cells with MEK5 knockdown (Fig. 3d). Unlike DNA-PKcs, ATM activation in response to phleomycin was independent of MEK5 in both cell lines. Collectively, these results show that MEK5 is required for full activation of DNA-PKcs in response to DSB genotoxic stress, and thus MEK5 acts upstream of DNA-PKcs. However, ATM activation is independent of MEK5.

**MEK5 ablation delays IR-induced foci resolution**

An early response to DSBs is phosphorylation of H2AX, a variant of histone H2A, at serine 139, which is carried out by both ATM and DNA-PKcs [3]. Phosphorylated H2AX, called γH2AX, spreads from the double strand break over several megabases, and this can be visualized as foci by immunofluorescence using phospho-Ser139 antibodies. Similar to H2AX, 53BP1 is recruited to break sites and co-localizes with γHA2X. 53BP1 has been shown to be important for DNA repair by NHEJ [29]. To gain further insight into how MEK5 depletion sensitizes

cells to genotoxic stress, we monitored the kinetics of γH2AX and 53BP1 foci formation in PC3 cells after exposure to 3 Gy γ-rays. The number of foci in unirradiated cells was low and it did not change with MEK5 silencing. As expected, radiation induced a rapid γH2AX and 53BP1 foci formation reaching maximum number within 30 min (Fig. 4a, c, d). MEK5 depletion (Fig. 4b) did not change the initial appearance of foci numbers. Subsequently, foci numbers in control PC3 cells were markedly diminished 2 h post-irradiation and returned to basal levels by 24 h. However, MEK5-depleted cells significantly delayed resolution of foci and they persisted above basal levels even after 48 h (Fig. 4a, c, d). We repeated the immunofluorescence experiments using transient *Luciferase* and *MEK5* siRNA transfection of PC3 cells with comparable results (Supplementary Fig. 8). Finally, we exposed PC3 cells to 10 μM etoposide and monitored H2AX and 53BP1 foci formation and resolution. In agreement with the IR treatment, exposure to etoposide resulted in increased number of foci at 30 min and 2 h, comparable for both control and MEK5 knockdown PC3 cells (Fig. 5a, b, c). However, foci resolution occurred much faster in control cells than in MEK5 silenced cells. We conclude that although the initial response to DNA damage is not dependent on MEK5 presence, the resolution and thus DNA repair of the damage is markedly delayed by MEK5 knockdown.

**MEK5 knockdown impairs non-homologous end joining**

Next, we performed experiments to test directly the ability of MEK5 to promote NHEJ by using a cell-based assay [30, 31]. pEGFP-N1 plasmid (Clontech) was digested with HindIII restriction endonuclease and transfected into PC3 cells expressing normal or reduced levels of MEK5. As a control, we treated PC3 cells with 2 μM NU7441, a DNA-PKcs-specific inhibitor. Transient transfection efficiency with the initial uncut plasmid was approximately 30% for PC3, PC3/*shMEK5*, and PC3/NU7441 cells as judged by the number of EGFP fluorescent cells measured under the microscope (Fig. 6a). Transiently transfected digested plasmid into PC3 cells resulted in approximately 10% of green fluorescent cells that express the protein. In contrast, PC3/*shMEK5* produced almost 7 times fewer EGFP-expressing cells (1.5%), whereas the proportion of EGFP-positive cells after treatment with NU7441 was approximately 1% (Fig. 6b). Thus, MEK5 downregulation impairs NHEJ.

**Combination of MEK5 blockade and ionizing radiation impairs tumor growth *in vivo***

To evaluate the efficacy of MEK5 knockdown combined with radiation to inhibit the growth of prostate cancer cells in mouse xenografts, we injected mice subcutaneously with PC3 cells expressing either *shControl* or *shMEK5#12*. We chose *shMEK5* clone 12, as this clone showed the greater efficiency in downregulating endogenous MEK5 and, *in vitro* proliferation assays showed no appreciable difference in cell proliferation between *shControl* and *shMEK5* PC3 cells (Supplementary Fig. 9). Mice bearing subcutaneous *shControl* or *shMEK5* xenografts were either left untreated or exposed to a single dose of 4 Gy, delivered specifically to the tumor by the Small Animal Radiation Research Platform (SARRP) irradiator using the onboard imager of the SARRP for image guided localization of the tumor (Supplementary Fig. 10) [32]. In agreement with *in vitro* proliferation assay, unirradiated *shMEK5* cell growth showed a small but not significant ($p = 0.5$) impairment of growth when compared with unirradiated *shControl* cell growth. Likewise, exposure of *shControl* tumors to 4 Gy γ-rays had no effect on tumor growth compared with unirradiated *shControl* tumors ($p = 0.5$; Fig. 7). In contrast, *shMEK5* cells exposed to radiation grew five-fold more slowly compared with unirradiated *shMEK5* cells ($p < 1E-04$) (Fig. 7). In summary, these findings demonstrate that whereas MEK5 depletion or IR used separately have only a moderate impact on PC3 cells grown in mouse xenografts, the combination of MEK5 blockade with IR leads to a dramatic inhibition of tumor growth.

**Discussion**

In this study, we identified a critical role of MEK5 in mediating resistance to DNA damaging agents, such as ionizing radiation and etoposide, in prostate cancer cells. Our *in vitro* and *in vivo* investigations demonstrate that MEK5 silencing sensitized PC3 and DU145 aggressive prostate cancer cell lines to IR, etoposide, and phleomycin through inactivation of DNA-PKcs and NHEJ repair. In contrast, neither EP156T nor LNCaP cell lines were affected by MEK5 knockdown, most likely because these cells express relatively lower protein levels compared with PC3 and DU145. Furthermore, in the androgen receptor (AR)-positive LNCaP cells, AR drives DNA-PKcs

expression and activation in response to genotoxic stress [33, 34]. As a result, LNCaP cells possess much higher levels of DNA-PKcs and active NHEJ. Thus, enhanced activity of DNA-PKcs combined with lower levels of MEK5 protein in LNCaP cells could preclude MEK5 from regulating DNA-PKcs phosphorylation levels.

While ATM is activated by IR, etoposide, or phleomycin equally well between control and MEK5 knockdown cells, MEK5 silencing impairs phosphorylation of DNA-PKcs at S2056 and T2609 in response to genotoxic stress, indicating reduced activation. We find that the combination of MEK5 abrogation with etoposide has a greater impact on prostate cancer cell survival than radiation. Etoposide treatment generates DSBs that are mainly repaired by NHEJ [35]. In contrast, IR creates DSBs that are repaired by both NHEJ and HR [35]. Thus, MEK5 ablation that diminishes DNA-PKcs phosphorylation and impairs NHEJ is expected to significantly reduce cell survival, when combined with etoposide.

It has been shown that IR-induced DNA-PKcs autophosphorylation at S2056 is regulated in a cell cycle-dependent manner with attenuated phosphorylation in the S phase [8]. However, we confirmed that MEK5 silencing had no impact on cell cycle distribution and neither altered cell cycle arrest after IR. It is well established that elevated DNA-PKcs activity in various human cancers results in increased resistance to DNA damage. DNA-PKcs is associated with poor disease outcome [36] and predicts response to radiotherapy in advanced prostate cancer [37, 38], whereas knockdown of DNA-PKcs sensitizes DU145 and PC3 cells to ionizing radiation [39]. However, DNA-PKcs is a ubiquitously expressed protein and its inhibition is expected to sensitize both normal epithelial and malignant prostate cells to radiation. In contrast, MEK5 is predominantly expressed in prostate cancer cells and thus targeting MEK5 would radiosensitize mainly tumor cells.

DSB generated by IR result in the formation of γH2AX and 53BP1 foci, and persistence of γH2AX foci indicate delayed repair and correlates with radiosensitivity [40-42]. The initial generation of IR-induced γH2AX and 53BP1 foci formation was similar between MEK5 knockdown and control cells. This can be attributed to ATM activation, which is known to play a dominant role in the generation of γH2AX, at least at early times post-irradiation [43]. In contrast, the resolution and thus repair of damage foci was markedly delayed in MEK5 knockdown cells compared with control cells. This is consistent with impaired DNA-PKcs action [43].

Furthermore, cell-based assays confirmed that NHEJ activity was significantly compromised in MEK5 knockdown cells.

In the current study, we provide evidence for the first time that a member of the MAP kinase family, MEK5, has an impact on DNA-PKcs phosphorylation and NHEJ repair in response to genotoxic stress. Members of the mitogen-activated protein kinases (MAPK) family, especially the MEK1/2/ERK1/2 pathway, have been functionally associated with tumor DNA damage response and repair pathway, albeit with variable outcomes. Thus, activation of ATM by radiation downregulates phospho-ERK1/2, and this downregulation is associated with radioresistance in human squamous cell carcinoma cell lines [44]. Similarly, ERK1/2 activation in response to etoposide, which is abrogated in ATM knockout cells, leads to increased apoptosis and sensitization to the drug [45]. In contrast, ATM inhibition partly blocks phospho-ERK1/2 and diminishes HR in response to radiation, whereas inhibition of ERK1/2 activity reduced phosphorylation of ATM at S1981 in glioma cells [46]. Furthermore, treatment of pancreatic cancer cells with the MEK1/2-specific inhibitor trametinib resulted in significant radiosensitization by suppressing both HR and NHEJ [47]. In this case, it was noted that total DNA-PKcs levels were reduced in the trametinib-treated cells. However, inhibition of ERK1/2 has also been shown to increase DNA-PKcs activation and promote DSB repair by NHEJ in response to etoposide in breast cancer cells [48]. In our study, ERK1/2 activation in response to IR was not detected in PC3 cells (unpublished results). However, EGF treatment of PC3 cells was able to induce phospho-ERK1/2, implying that the MEK1/2/ERK1/2 pathway is intact in these cells. On the other hand, DU145 cells express active ERK1/2 constitutively and phospho-ERK1/2 levels were not further induced by IR. Recently a study was published that showed ERK5 confers radioresistance to lung adenocarcinoma cell lines [49]. However, the mode of action of ERK5 in response to IR differs significantly from the present study. Thus, whereas ERK5 knockdown combined with radiation leads to compromised G2/M cell cycle arrest, our results show that MEK5 downregulation does not affect the cell cycle checkpoint response. Moreover, it was shown that IR caused sustained activation of ERK5, whereas we find that activation of ERK5 in prostate cancer cells is fast and transient, reaching maximal levels of phosphorylation at around 10-30 min, diminishing thereafter and becoming undetectable by 2 hr post-irradiation. These differences

may be attributed to different cancer types or, alternatively, to the fact that ERK5 has additional, MEK5-independent functions, and thus the impact of MEK5 knockdown may differ from that of ERK5 depletion [50].

In conclusion, our results support the mechanism that MEK5 inhibition sensitizes prostate cancer cells to genotoxic stress by severely impairing DNA-PKcs autophosphorylation and DNA repair by NHEJ. Our i*n vivo* experiments show that downregulation of MEK5 combined with irradiation markedly sensitizes prostate cancer cells to radiotherapy and support targeting MEK5 as a potential clinical intervention for intermediate and high-risk prostate cancer patients treated with radiotherapy.

## Materials and methods

Detailed experimental procedures describing cell culture, cell proliferation assays, irradiation, clonogenic survival assay, RNA interference and plasmid construction, cell cycle analysis, Western blot analysis, immunofluorescence, NHEJ assay, animal studies, and statistical analysis are included in the Supplementary Materials and Methods document.

## Acknowledgements

This work is supported by the Department of Defense Prostate Cancer Research Program, W81XWH-15-1-0296 (CGB). This study also used the resources of the Herbert Irving Comprehensive Cancer Center Flow Cytometry, Radiation Research, and Confocal and Specialized Microscopy Shared Resources funded in part through Center Grant P30CA013696. We thank Theresa Swayne and Laura Munteanu from the Confocal and Specialized Microscopy Shared Resource of the Irving Cancer Research Center (ICRC) and Drs. Siu-Hong Ho, Wei Wang, and Caisheng Lu from the Flow Cytometry Shared Resource of the Herbert Irving Comprehensive Cancer Center at Columbia University Irving Medical Center for their help in performing the immunofluorescence and flow cytometry experiments.

**Compliance with Ethical Standards**

**Conflict of Interest**: The authors declare that they have no conflict of interest.

**References**


1. Bolla M, Van Tienhoven G, Warde P, Dubois JB, Mirimanoff RO, Storme G, *et al*. External irradiation with or without long-term androgen suppression for prostate cancer with high metastatic risk: 10-year results of an EORTC randomised study. Lancet Oncol. 2010;11(11):1066-1073.
2. Palacios DA, Miyake M, Rosser CJ. Radiosensitization in prostate cancer: mechanisms and targets. BMC Urol. 2013;13:4.
3. Ciccia A, Elledge SJ. The DNA damage response: making it safe to play with knives. Mol Cell. 2010;40(2):179-204.
4. San Filippo J, Sung P, Klein H. Mechanism of eukaryotic homologous recombination. Annu Rev Biochem. 2008;77:229-257.
5. Lieber MR. The mechanism of human nonhomologous DNA end joining. J Biol Chem. 2008;283(1):1-5.
6. Jeggo PA.DNA breakage and repair. Adv Genet. 1998;38:185-218.
7. Davis AJ, Chen BP, Chen DJ. DNA-PK: a dynamic enzyme in a versatile DSB repair pathway. DNA Repair (Amst). 2014;17:21-29.
8. Chen BP, Chan DW, Kobayashi J, Burma S, Asaithamby A, Morotomi-Yano K, *et al*. Cell cycle dependence of DNA-dependent protein kinase phosphorylation in response to DNA double strand breaks. J Biol Chem. 2005;280(15):14709-14715.
9. Zhou G, Bao ZQ, Dixon JE. Components of a new human protein kinase signal transduction pathway. J Biol Chem. 1995:270(21):12665-12669.
10. Sun W, Kesavan K, Schaefer BC, Garrington TP, Ware M, Johnson NL, *et al*. MEKK2 associates with the adapter protein Lad/RIBP and regulates the MEK5-BMK1/ERK5 pathway. J Biol Chem. 2001:276(7):5093-5100.

11. Chao TH, Hayashi M, Tapping RI, Kato Y, Lee JD. MEKK3 directly regulates MEK5 activity as part of the big mitogen-activated protein kinase 1 (BMK1) signaling pathway. J Biol Chem. 1999:274(51):36035-36038.
12. Suzaki Y, Yoshizumi M, Kagami S, Koyama AH, Taketani Y, Houchi H, *et al*. Hydrogen peroxide stimulates c-Src-mediated big mitogen-activated protein kinase 1 (BMK1) and the MEF2C signaling pathway in PC12 cells: potential role in cell survival following oxidative insults. J Biol Chem. 2002:277(11):9614-9621.
13. Arnoux V, Nassour M, L'Helgoualc'h A, Hipskind RA, Savagner P. Erk5 controls Slug expression and keratinocyte activation during wound healing. Mol Biol Cell. 2008:19(11):4738-47349.
14. Zhou C, Nitschke AM, Xiong W, Zhang Q, Tang Y, Bloch M, *et al*. Proteomic analysis of tumor necrosis factor-alpha resistant human breast cancer cells reveals a MEK5/Erk5-mediated epithelial-mesenchymal transition phenotype. Breast Cancer Res. 2008:10(6):R105.
15. Schweppe RE, Cheung TH, Ahn NG. Global gene expression analysis of ERK5 and ERK1/2 signaling reveals a role for HIF-1 in ERK5-mediated responses. J Biol Chem. 2006:281(30):20993-21003.
16. English JM, Vanderbilt CA, Xu S, Marcus S, Cobb MH. Isolation of MEK5 and differential expression of alternatively spliced forms. J Biol Chem. 1995;270(48):28897-288902.
17. Seyfried J, Wang X, Kharebava G, Tournier C. A novel mitogen-activated protein kinase docking site in the N terminus of MEK5alpha organizes the components of the extracellular signal-regulated kinase 5 signaling pathway. Mol Cell Biol. 2005;25(22):9820-9828.
18. Cameron SJ, Abe J, Malik S, Che W, Yang J. Differential role of MEK5alpha and MEK5beta in BMK1/ERK5 activation. J Biol Chem. 2004;279(2):1506-1512.
19. Tusa I, Gagliardi S, Tubita A, Pandolfi S, Urso C, Borgognoni L, *et al*. ERK5 is activated by oncogenic BRAF and promotes melanoma growth. Oncogene. 2018;37(19):2601-2614.

20. Benito-Jardón L, Díaz-Martínez M, Arellano-Sánchez N, Vaquero-Morales P, Esparís-Ogando A, Teixidó J. Resistance to MAPK Inhibitors in Melanoma Involves Activation of the IGF1R-MEK5-Erk5 Pathway. Cancer Res. 2019;79(9):2244-2256.
21. Ghosh AK, Steele R, Ray RB. c-myc Promoter-binding protein 1 (MBP-1) regulates prostate cancer cell growth by inhibiting MAPK pathway. J Biol Chem. 2005;280(14):14325-14330.
22. Regan CP, Li W, Boucher DM, Spatz S, Su MS, Kuida K. Erk5 null mice display multiple extraembryonic vascular and embryonic cardiovascular defects. Proc Natl Acad Sci U S A. 2002;99(14):9248-9253.
23. Yan L, Carr J, Ashby PR, Murry-Tait V, Thompson C, Arthur JS. Knockout of ERK5 causes multiple defects in placental and embryonic development. BMC Dev Biol. 2003;3:11.
24. Loveridge CJ, Mui EJ, Patel R, Tan EH, Ahmad I, Welsh M, *et al*. Increased T-cell Infiltration Elicited by Erk5 Deletion in a Pten-Deficient Mouse Model of Prostate Carcinogenesis. Cancer Res. 2017;77(12):3158-3168.
25. Mehta PB, Jenkins BL, McCarthy L, Thilak L, Robson CN, Neal DE, *et al*. MEK5 overexpression is associated with metastatic prostate cancer, and stimulates proliferation, MMP-9 expression and invasion. Oncogene. 2003;22(9):1381-1389.
26. McCracken SR, Ramsay A, Heer R, Mathers ME, Jenkins BL, Edwards J, *et al*. Aberrant expression of extracellular signal-regulated kinase 5 in human prostate cancer. Oncogene. 2008;27(21):2978-2988.
27. Ramsay AK, McCracken SR, Soofi M, Fleming J, Yu AX, Ahmad I, *et al*. ERK5 signalling in prostate cancer promotes an invasive phenotype. Br J Cancer. 2011;104(4):664-672.
28. Adachi N, Suzuki H, Liizumi S, Koyama H. Hypersensitivity of nonhomologous DNA end-joining mutants to VP-16 and ICRF-193: implications for the repair of topoisomerase II-mediated DNA damage. J Biol Chem. 2003;278:35897–35902.
29. Panier S, Durocher D. Push back to respond better: regulatory inhibition of the DNA double-strand break response. Nat Rev Mol Cell Biol. 2013;14(10):661-672.

30. Wang HC, Chou WC, Shieh SY, Shen CY. Ataxia telangiectasia mutated and checkpoint kinase 2 regulate BRCA1 to promote the fidelity of DNA end-joining. Cancer Res. 2006;66(3):1391-400.
31. Kim MR, Lee J, An YS, Jin YB, Park IC, Chung E, *et al*. TGFβ1 protects cells from γ-IR by enhancing the activity of the NHEJ repair pathway. Mol Cancer Res. 2015;13(2):319-329.
32. Wu CC, Chaudhary KR, Na YH, Welch D, Black PJ, Sonabend AM, *et al*. Quality Assessment of Stereotactic Radiosurgery of a Melanoma Brain Metastases Model Using a Mouselike Phantom and the Small Animal Radiation Research Platform. Int J Radiat Oncol Biol Phys. 2017;99(1):191-201.
33. Polkinghorn WR, Parker JS, Lee MX, Kass EM, Spratt DE, Iaquinta PJ, et al. Androgen receptor signaling regulates DNA repair in prostate cancers. Cancer Discov. 2013;3(11):1245-53.
34. Goodwin JF, Schiewer MJ, Dean JL, Schrecengost RS, de Leeuw R, Han S, et al. A hormone-DNA repair circuit governs the response to genotoxic insult. Cancer Discov. 2013;3(11):1254-71.
35. Shibata A, Conrad S, Birraux J, Geuting V, Barton O, Ismail A, et al. Factors determining DNA double-strand break repair pathway choice in G2 phase. EMBO J. 2011;30(6):1079-92.
36. Brenner JC, Ateeq B, Li Y, Yocum AK, Cao Q, Asangani IA, *et al*. Mechanistic rationale for inhibition of poly(ADP-ribose) polymerase in ETS gene fusion-positive prostate cancer. Cancer Cell. 2011;19(5):664-678.
37. Ni X, Zhang Y, Ribas J, Chowdhury WH, Castanares M, Zhang Z, *et al*. Prostate-targeted radiosensitization via aptamer-shRNA chimeras in human tumor xenografts. J Clin Invest. 2011;121(6):2383-2390.
38. Bouchaert P, Guerif S, Debiais C, Irani J, Fromont G. DNA-PKcs expression predicts response to radiotherapy in prostate cancer. Int J Radiat Oncol Biol Phys. 84(5):1179-1185.
39. Collis SJ, Swartz MJ, Nelson WG, DeWeese TL. Enhanced radiation and chemotherapy-mediated cell killing of human cancer cells by small inhibitory RNA silencing of DNA repair factors. Cancer Res. 2003;63(7):1550-1554.

40. Banáth JP, Macphail SH, Olive PL. Radiation sensitivity, H2AX phosphorylation, and kinetics of repair of DNA strand breaks in irradiated cervical cancer cell lines. Cancer Res. 2004;64(19):7144-7149.
41. Olive PL, Banáth JP. Phosphorylation of histone H2AX as a measure of radiosensitivity. Int J Radiat Oncol Biol Phys. 2004;58(2):331-335.
42. Taneja N, Davis M, Choy JS, Beckett MA, Singh R, Kron SJ, *et al*. Histone H2AX phosphorylation as a predictor of radiosensitivity and target for radiotherapy. J Biol Chem. 2004;279(3):2273-2280.
43. Stiff T, O'Driscoll M, Rief N, Iwabuchi K, Löbrich M, Jeggo PA. ATM and DNA-PK function redundantly to phosphorylate H2AX after exposure to ionizing radiation. Cancer Res. 2004 1;64(7):2390-2396.
44. Nyati MK, Feng FY, Maheshwari D, Varambally S, Zielske SP, Ahsan A, *et al*. Ataxia telangiectasia mutated down-regulates phospho-extracellular signal-regulated kinase 1/2 via activation of MKP-1 in response to radiation. Cancer Res. 2006;66(24):11554-9.
45. Tang D, Wu D, Hirao A, Lahti JM, Liu L, Mazza B, *et al*. ERK activation mediates cell cycle arrest and apoptosis after DNA damage independently of p53. J Biol Chem. 2002;277(15):12710-12717.
46. Golding SE, Rosenberg E, Neill S, Dent P, Povirk LF, Valerie K. Extracellular signal-related kinase positively regulates ataxia telangiectasia mutated, homologous recombination repair, and the DNA damage response. Cancer Res. 2007;67(3):1046-1053.
47. Estrada-Bernal A, Chatterjee M, Haque SJ, Yang L, Morgan MA, Kotian S, *et al*. MEK inhibitor GSK1120212-mediated radiosensitization of pancreatic cancer cells involves inhibition of DNA double-strand break repair pathways. Cell Cycle. 2015;14(23):3713-3724.
48. Wei F, Yan J, Tang D, Lin X, He L, Xie Y, *et al*. Inhibition of ERK activation enhances the repair of double-stranded breaks via non-homologous end joining by increasing DNA-PKcs activation. Biochim Biophys Acta. 2013;1833(1):90-100.

49. Jiang W, Jin G, Cai F, Chen X, Cao N, Zhang X, *et al*. Extracellular signal-regulated kinase 5 increases radioresistance of lung cancer cells by enhancing the DNA damage response. Exp Mol Med. 2019;51(2):19.
50. Pavan S, Meyer-Schaller N, Diepenbruck M, Kalathur RKR, Saxena M, Christofori G. A kinome-wide high-content siRNA screen identifies MEK5-ERK5 signaling as critical for breast cancer cell EMT and metastasis. Oncogene. 2018;37(31):4197-4213.

**Figure legends**

**Fig. 1** MEK5 silencing sensitizes cells to radiation. **a** DU145 cells were transiently transfected with *Luciferase* (siLUC) or *MEK5* (siMEK5-78) siRNA. Two days later, cells were serum-starved for 24h and irradiated by various doses of γ-radiation. Fifteen minutes later, cells were lysed and proteins were subjected to immunoblotting with the indicated antibodies. **b** Time course activation of ERK5 in response to ionizing radiation. PC3 cells were transiently transfected with either *Luciferase* (siLUC) or *MEK5* (siMEK5-10) siRNA and serum starved for 48h. Cells were irradiated with 4 Gy and lysed at the indicated time points. Levels of total MEK5 and α-tubulin are shown. **c** PC3 stably expressing a scrambled (*shControl*) or *MEK5* (clone#12) shRNA were irradiated with 3 Gy γ-rays and immunoblotted subsequently with phospho-ERK5, total ERK5, MEK5, and α-tubulin antibodies. **d** DU145 clonogenic survival assay. DU145 cells were either left untransfected (DU) or transiently transfected with luciferase siRNA (DL) or four different siRNAs against MEK5 (D76, D78, D10, D20). Two days later, cells were irradiated with increasing doses of γ-radiation and plated for clonogenic assay. **e** PC3 cells were transfected with luciferase siRNA (PL) as control or MEK5 siRNAs (P76, P78) and clonogenic assay was carried out as in d. **f** Cell proliferation assay. DU145 and PC3 cells were transiently transfected with control *Luciferase* (LUC) or *MEK5* (D78 or P78) siRNA. Three days later, cells were irradiated with 4 Gy γ-rays and incubated for 6 days. Cells were trypsinized and counted with a hemocytometer. **g** DU145 and PC3 cells were stably expressing either scrambled (shControl) or *MEK5* (shMEK5) shRNA were exposed to 4 Gy (DU145) or 3 Gy (PC3), or were sham

irradiated. Data for d, e, and f represent the mean ± S.D (n = 3). P-values were calculated by Student's t-test. UI: unirradiated.

**Fig. 2** MEK5 knockdown impairs DNA-PKcs phosphorylation in response to ionizing radiation. PC3 (**a)** or DU145 (**b)** cells were transiently transfected with *Luciferase* siRNA (siLUC) or siRNAs against *MEK5* (#78). Four days later, cells were irradiated with 3 Gy γ-radiation, lysates were prepared at the indicated times and immunoblotted with the indicated antibodies. **c** PC3 cells stably expressing a control (shControl) or *MEK5* (clone#12, *upper*; clone#22, *lower*) shRNA were exposed to 3 Gy of γ-rays and cells were lysed at the indicated times. Lysates were immunoblotted sequentially with the indicated antibodies. **d** DU145 cells stable expressing a scrambled (*shControl*) or *MEK5* (clone#7) shRNA were exposed to 3 Gy of γ-rays and cells were lysed at different times and immunoblotted sequentially with anti-phospho-DNA-PKcs (S2056) and anti-total DNA-PKcs antibodies. **e** Ectopic expression of MEK5 restores activation of DNA-PKcs. PC3 cells stably expressing *shControl*, *shMEK5* (clone#12), or *shMEK5* transiently expressing MEK5-pcDNA3 vector were exposed to 3 Gy of γ-rays and lysed at the indicated times. Lysates were immunoblotted sequentially with phospho-DNA-PKcs (Ser2056), total DNA-PKcs, phospho-ATM (Ser1981) and total ATM antibodies. UI: unirradiated.

**Fig. 3** MEK5 knockdown impairs DNA-PKcs phosphorylation in response to etoposide and phleomycin. **a** dose response curves of control and *MEK5* shRNA in PC3 cells exposed to increasing concentrations of etoposide. Cell numbers were recorded 6 days post-treatment. **b** PC3 cells were exposed to 10 μM etoposide for 16 h, drug was removed, and cells were incubated for 6 days. Subsequently, cells were fixed, stained with crystal violet, quantified and expressed as percentage of the shControl-treated cells. Mean ± S.D. (n = 3). P-value were calculated by Student's t-test**. c** PC3 cells stably expressing a scrambled (*shControl*) or *MEK5* (clone #12) shRNA were treated with 10 μM etoposide, cells were lysed at the indicated times and immunoblotted sequentially with the indicated antibodies. **d** PC3 cells (*left*) stably expressing *shControl* or *shMEK5* (clone #12) and DU145 cells (*right*) stably expressing *shControl* or *shMEK5* (clone #9) were treated with 60 μg/ml phleomycin for 2 h, drug

was removed and cells were incubated for the indicated times. Lysates were immunoblotted with the indicated antibodies. UT: untreated.

**Fig. 4** MEK5 knockdown delays resolution of irradiation-induced DSBs. PC3 cells stably expressing *shControl* or *shMEK5* were exposed to 3 Gy γ-rays, fixed and stained for γH2AX, 53BP1, and 4', 6-diamidino-2-phenylindole (DAPI; DNA). **a** Representative images and **b** western blot analysis of MEK5 protein levels in *shControl* and *shMEK5* (clone #12) cells. **c, d** quantitation of number of γH2AX (c) and 53BP1 (d) foci per cell over time after irradiation between cells expressing *shControl* and *shMEK5.* Shown mean ± S.D. (n = 3). * $p < 0.001$, calculated by Student's t-test. UI: unirradiated.

**Fig. 5** MEK5 knockdown delays resolution of etoposide-induced DSBs. PC3 cells stably expressing *shControl* or *shMEK5* were treated with etoposide and, at the indicated times, they were fixed and stained for γH2AX, 53BP1, and 4', 6-diamidino-2-phenylindole (DAPI; DNA). **a** Representative images and **b, c** quantitation of number of γH2AX (b) and 53BP1 (c) foci per cell over time after etoposide treatment between cells expressing *shControl* and *shMEK5*. Shown mean ± S.D. (n = 3). * $p < 0.001$, calculated by Student's t-test. UT: untreated.

**Fig. 6** MEK5 depletion impairs non-homologous end joining. **a** intact or **b** HindIII-digested pEGFP-N1 vector was transiently transfected in PC3 cells expressing *shControl* or *shMEK5. shControl* cells were also treated or not with NU7441. Twenty-four hours post-transfection, cells were fixed, stained with DAPI, and EGFP-positive cells were quantitated by fluorescence as percent EGFP-positive cells/total (DAPI) number cells. Mean ± S.D. (n = 3). P-value was calculated by Student's t-test. UT: uncut plasmid; HindIII: restriction enzyme-digested plasmid.

**Fig. 7** MEK5 ablation synergizes with radiotherapy to suppress PC3 tumor growth *in vivo*. PC3 cells stably expressing scrambled (control) or *MEK5* (clone #12) shRNA were injected subcutaneously into athymic male

NU/J mice. When tumors reached ~200 $mm^3$, mice were irradiated with 4 Gy x-rays (IR), or they were sham irradiated. Tumor growth was measured using a caliper. Shown mean volume ± S.E.M. (n = 8 mice /treatment).

**Figure 1**

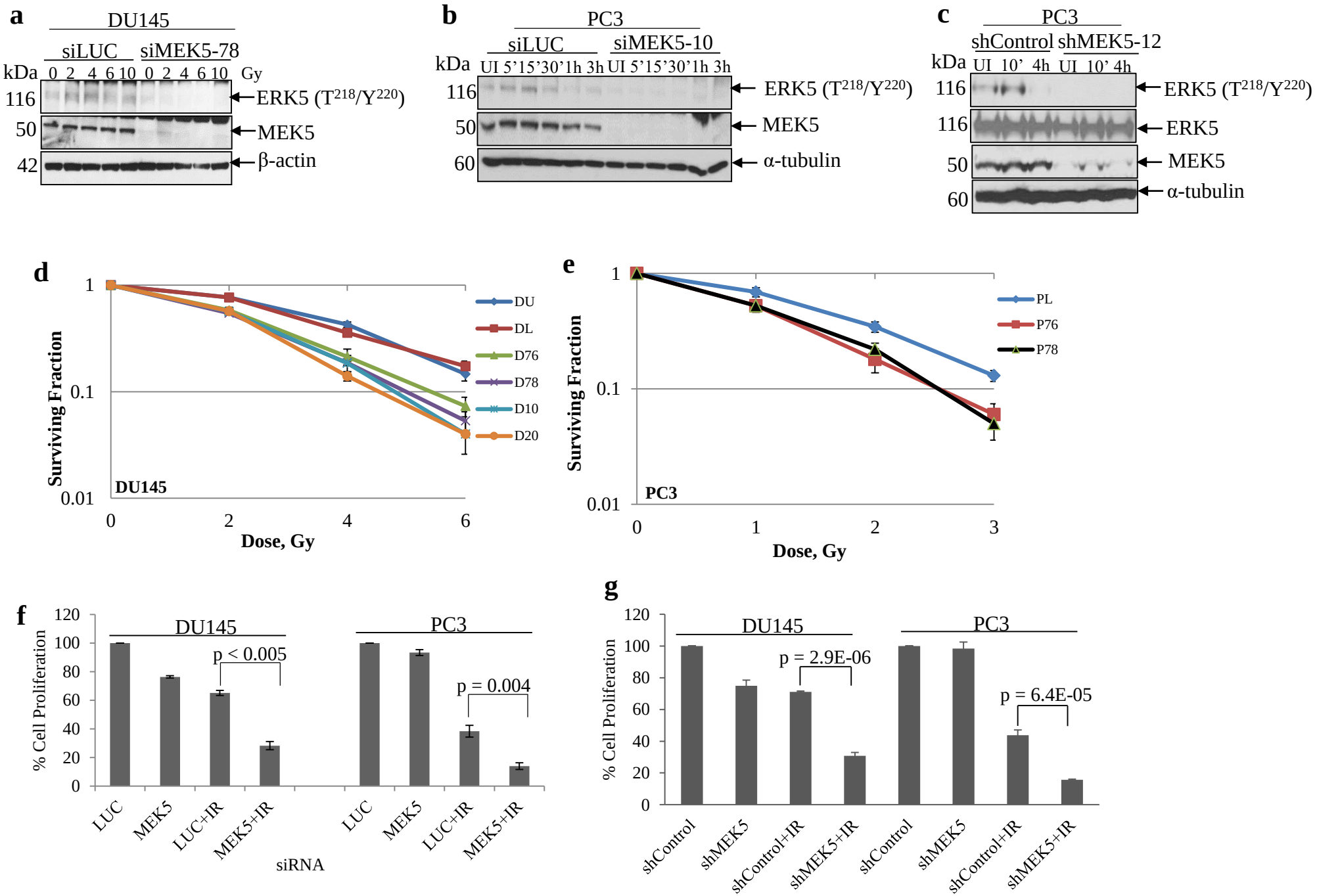
a
DU145
siLUC
siMEK5-78
kDa 0 2 4 6 10 0 2 4 6 10 Gy
116
50
42
ERK5 (T218/Y220)
MEK5
β-actin
b
PC3
siLUC
siMEK5-10
kDa UI 5'15'30'1h 3h UI 5'15'30'1h 3h
116
50
60
ERK5 (T218/Y220)
MEK5
α-tubulin
c
PC3
shControl
shMEK5-12
kDa UI 10' 4h UI 10' 4h
116
116
50
60
ERK5 (T218/Y220)
ERK5
MEK5
α-tubulin
d
Surviving Fraction
1
0.1
0.01
DU145
0
2
4
6
Dose, Gy
DU
DL
D76
D78
D10
D20
e
Surviving Fraction
1
0.1
0.01
PC3
0
1
2
3
Dose, Gy
PL
P76
P78
f
% Cell Proliferation
120
100
80
60
40
20
0
DU145
PC3
p < 0.005
p = 0.004
LUC
MEK5
LUC+IR
MEK5+IR
LUC
MEK5
LUC+IR
MEK5+IR
siRNA
g
% Cell Proliferation
120
100
80
60
40
20
0
DU145
PC3
p = 2.9E-06
p = 6.4E-05
shControl
shMEK5
shControl+IR
shMEK5+IR
shControl
shMEK5
shControl+IR
shMEK5+IR

**Figure 2**

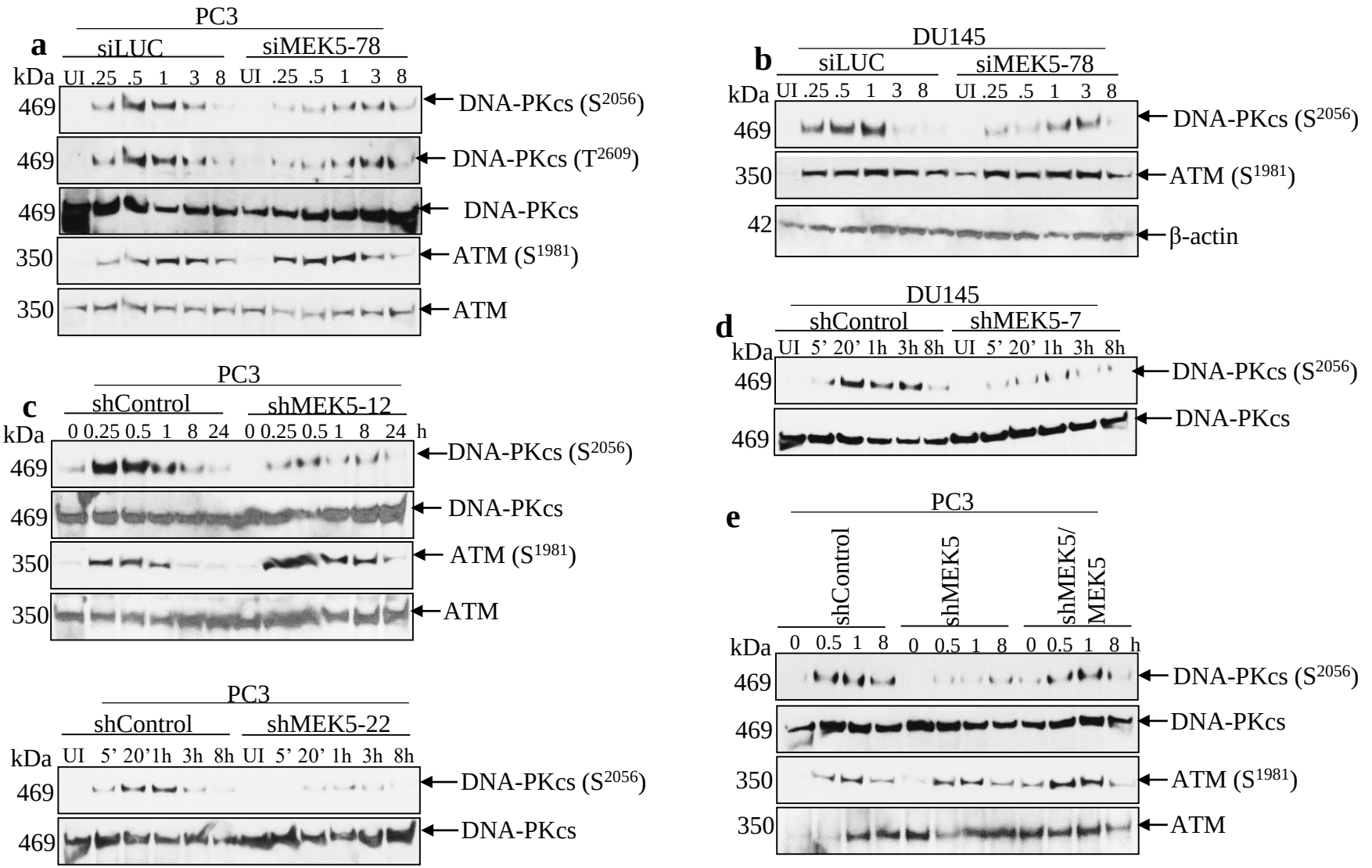
a
PC3
siLUC
siMEK5-78
kDa UI .25 .5 1 3 8 UI .25 .5 1 3 8
469 DNA-PKcs (S2056)
469 DNA-PKcs (T2609)
469 DNA-PKcs
350 ATM (S1981)
350 ATM
b
DU145
siLUC
siMEK5-78
kDa UI .25 .5 1 3 8 UI .25 .5 1 3 8
469 DNA-PKcs (S2056)
350 ATM (S1981)
42 β-actin
c
PC3
shControl
shMEK5-12
kDa 0 0.25 0.5 1 8 24 0 0.25 0.5 1 8 24 h
469 DNA-PKcs (S2056)
469 DNA-PKcs
350 ATM (S1981)
350 ATM
d
DU145
shControl
shMEK5-7
kDa UI 5' 20' 1h 3h 8h UI 5' 20' 1h 3h 8h
469 DNA-PKcs (S2056)
469 DNA-PKcs
e
PC3
shControl
shMEK5
shMEK5/ MEK5
kDa 0 0.5 1 8 0 0.5 1 8 0 0.5 1 8 h
469 DNA-PKcs (S2056)
469 DNA-PKcs
350 ATM (S1981)
350 ATM
PC3
shControl
shMEK5-22
kDa UI 5' 20'1h 3h 8h UI 5' 20' 1h 3h 8h
469 DNA-PKcs (S2056)
469 DNA-PKcs

**Figure 3**

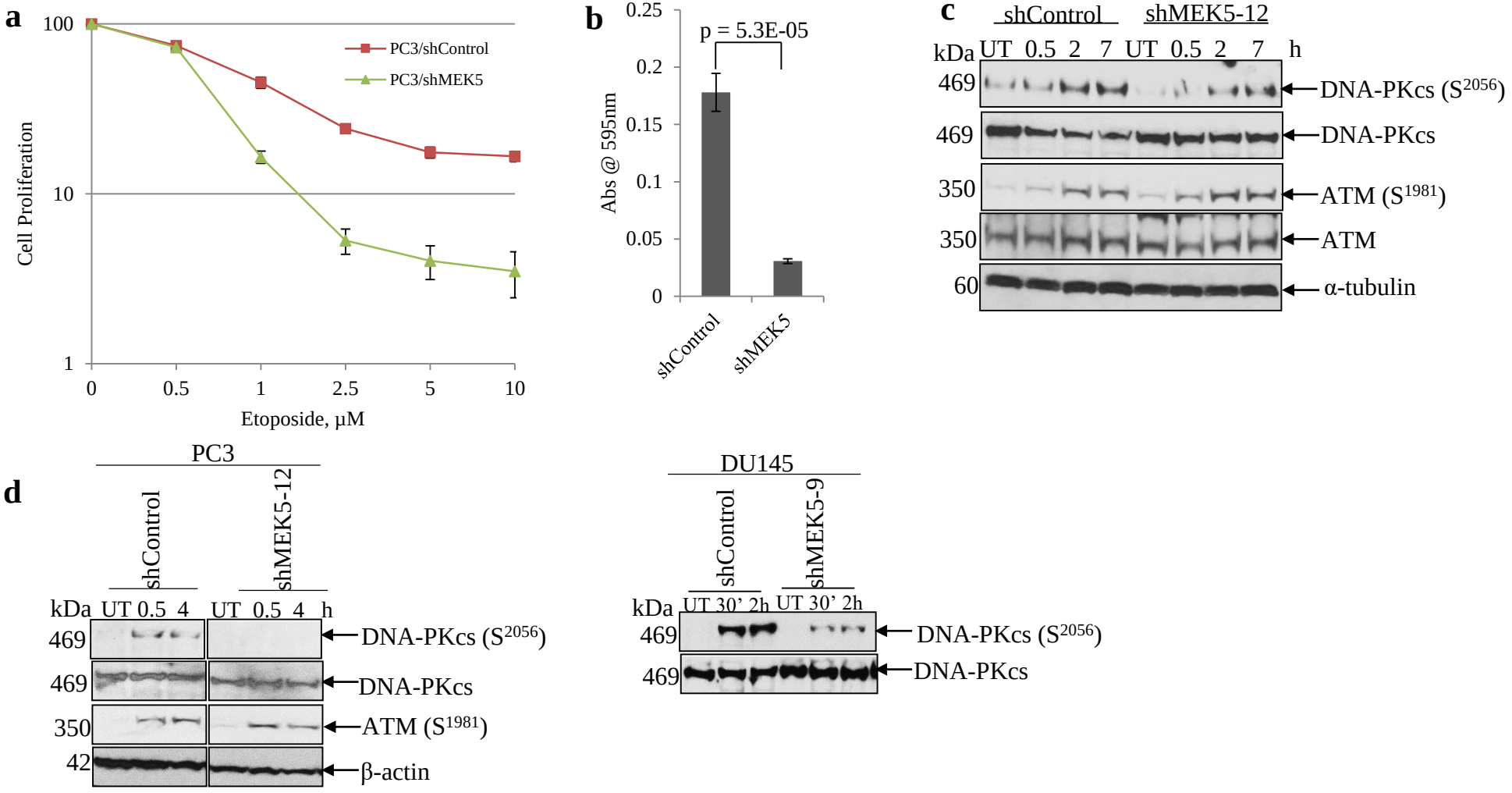
a
100
10
1
Cell Proliferation
PC3/shControl
PC3/shMEK5
0
0.5
1
2.5
5
10
Etoposide, μM
b
0.25
0.2
0.15
0.1
0.05
0
Abs @ 595nm
p = 5.3E-05
shControl
shMEK5
c
PC3
shControl
shMEK5-12
kDa UT 0.5 2 7 UT 0.5 2 7 h
469
DNA-PKcs (S2056)
469
DNA-PKcs
350
ATM (S1981)
350
ATM
60
α-tubulin
d
PC3
shControl
shMEK5-12
kDa UT 0.5 4 UT 0.5 4 h
469
DNA-PKcs (S2056)
469
DNA-PKcs
350
ATM (S1981)
42
β-actin
DU145
shControl
shMEK5-9
kDa UT 30' 2h UT 30' 2h
469
DNA-PKcs (S2056)
469
DNA-PKcs

Figure 4

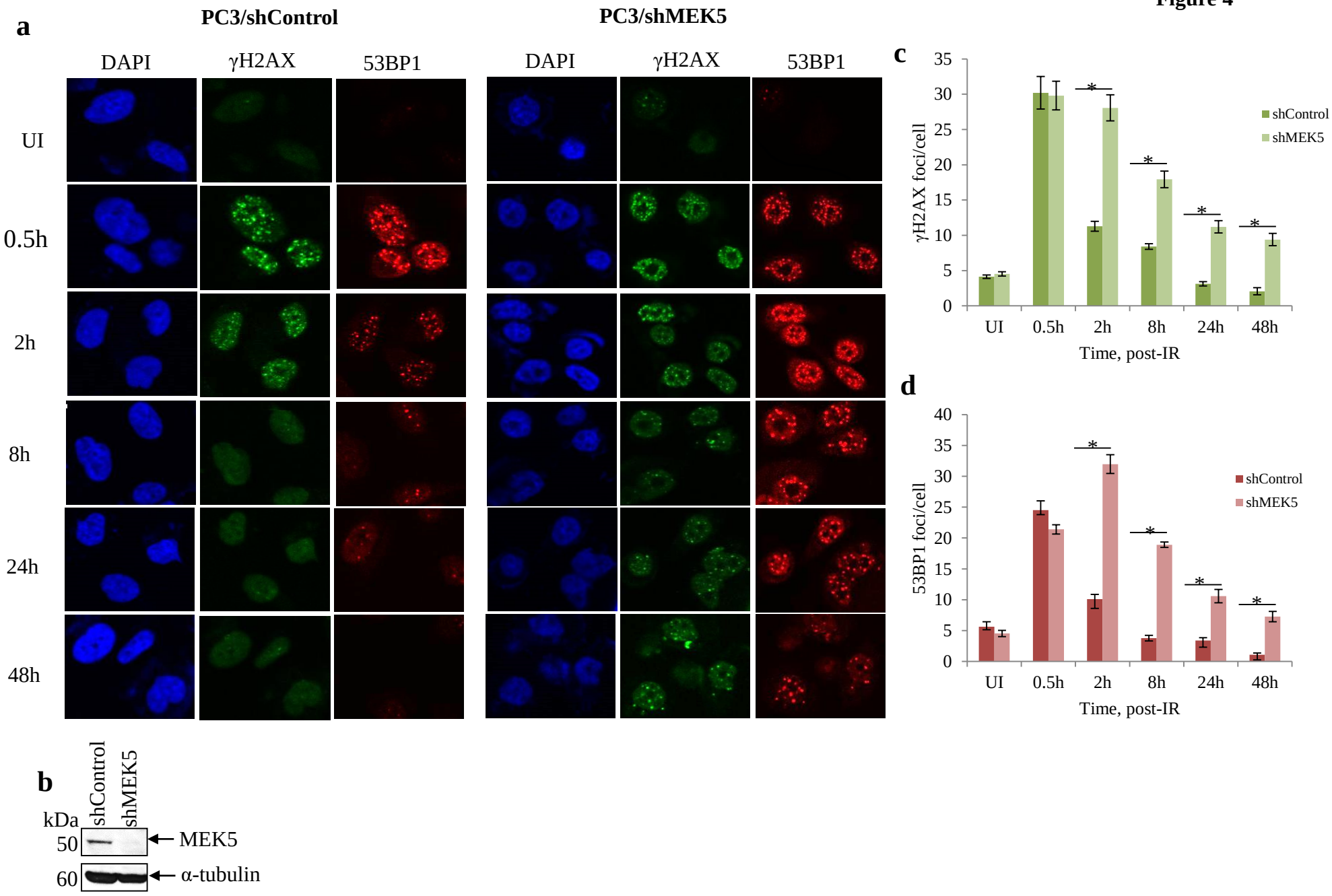
a
PC3/shControl
PC3/shMEK5
DAPI
γH2AX
53BP1
UI
0.5h
2h
8h
24h
48h
b
kDa
shControl
shMEK5
50
MEK5
60
α-tubulin
c
γH2AX foci/cell
shControl
shMEK5
Time, post-IR
d
53BP1 foci/cell
shControl
shMEK5
Time, post-IR

**Figure 5**

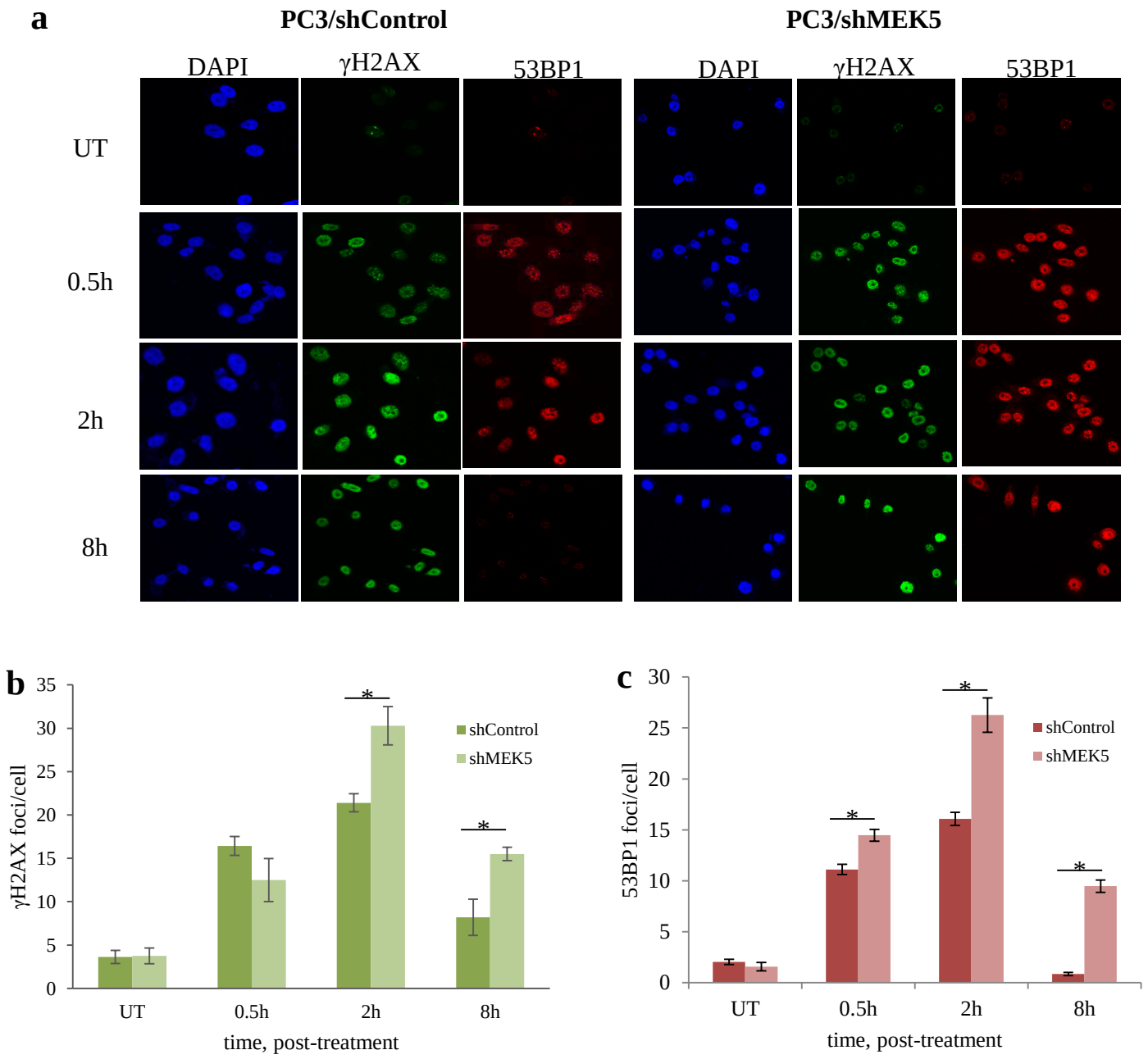
a
PC3/shControl
PC3/shMEK5
DAPI
γH2AX
53BP1
DAPI
γH2AX
53BP1
UT
0.5h
2h
8h
b
γH2AX foci/cell
35
30
25
20
15
10
5
0
*
*
shControl
shMEK5
UT
0.5h
2h
8h
time, post-treatment
c
53BP1 foci/cell
30
25
20
15
10
5
0
*
*
*
shControl
shMEK5
UT
0.5h
2h
8h
time, post-treatment

**Figure 6**

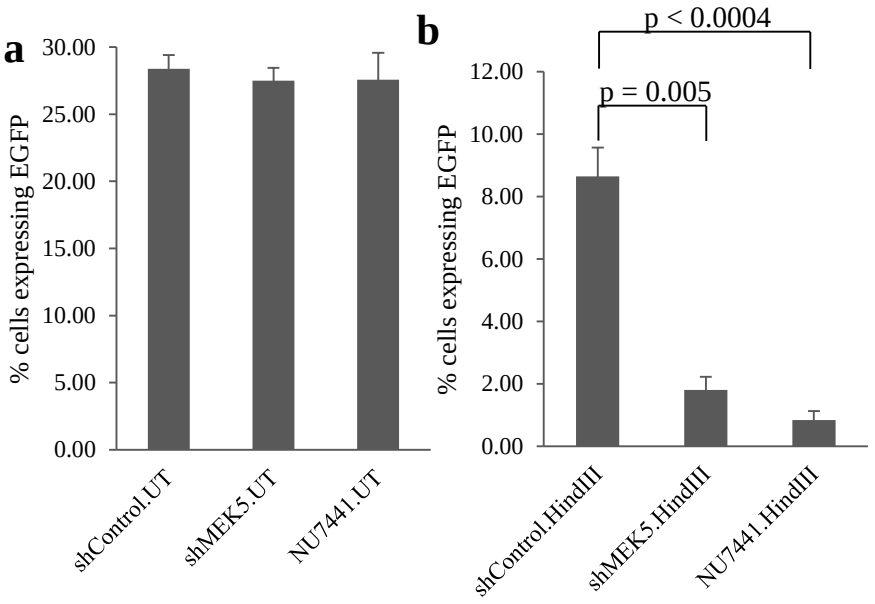
a
30.00
25.00
20.00
15.00
10.00
5.00
0.00
% cells expressing EGFP
shControl.UT
shMEK5.UT
NU7441.UT
b
p < 0.0004
p = 0.005
12.00
10.00
8.00
6.00
4.00
2.00
0.00
% cells expressing EGFP
shControl.HindIII
shMEK5.HindIII
NU7441.HindIII

**Figure 7**

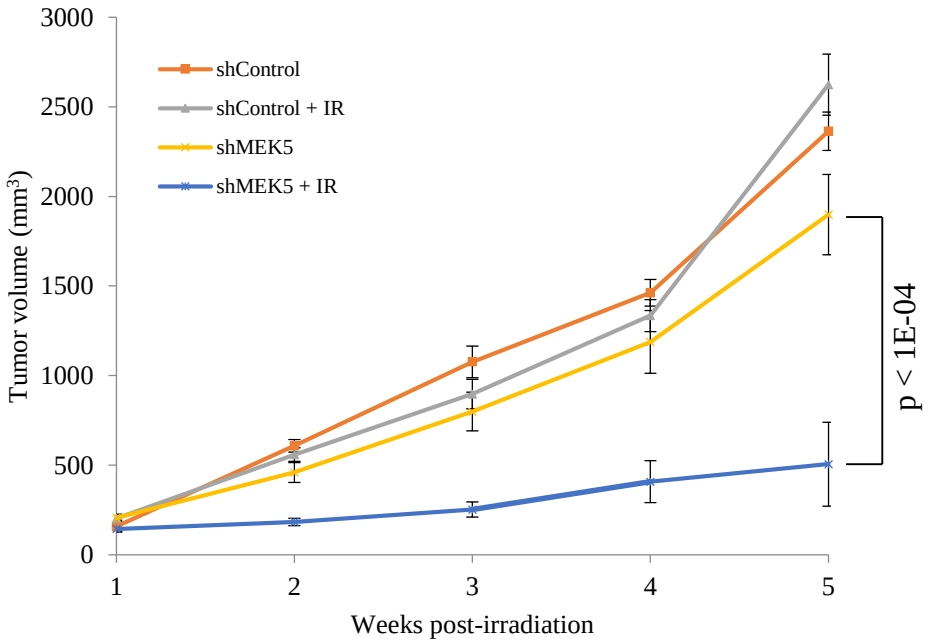
3000
2500
2000
1500
1000
500
0
Tumor volume (mm3)
shControl
shControl + IR
shMEK5
shMEK5 + IR
1
2
3
4
5
Weeks post-irradiation
p < 1E-04